

MACTAS: Self-Attention-Based Inter-Agent Communication in Multi-Agent Reinforcement Learning with Action-Value Function Decomposition

Maciej Wojtala^{1,2 *}, Bogusz Stefańczyk^{2 *}, Dominik Jacek Bogucki^{3,4 *},
 Łukasz Lepak⁵, Jakub Strykowski⁵ and Paweł Wawrzynski²

¹University of Warsaw

²IDEAS Research Institute

³Institute of Fundamental Technological Research, Polish Academy of Sciences

⁴IDEAS NCBR

⁵Warsaw University of Technology

mw406587@students.mimuw.edu.pl, bogusz.stefanczyk@ideas.edu.pl, dominik.bogucki@ideas-ncbr.pl,
 lukasz.lepak@pw.edu.pl, jakub.strykowskii@gmail.com, pawel.wawrzynski@ideas.edu.pl

Abstract

Communication is essential for the collective execution of complex tasks by human agents, motivating interest in communication mechanisms for multi-agent reinforcement learning (MARL). However, existing communication protocols in MARL are often complex and non-differentiable. In this work, we introduce a self-attention-based communication method that exchanges information between the agents in MARL. Our proposed approach is fully differentiable, allowing agents to learn to generate messages in a reward-driven manner. The method can be seamlessly integrated with any action-value function decomposition algorithm and can be viewed as an orthogonal extension of such decompositions. Notably, it includes a fixed number of trainable parameters, independent of the number of agents, which makes it scalable to large systems. Experimental results on the SMACv2 benchmark demonstrate the effectiveness of our approach, which achieves state-of-the-art performance on a number of maps.

1 Introduction

Multi-agent reinforcement learning (MARL) [Ning and Xie, 2024; Du and Ding, 2021; Nguyen *et al.*, 2020; Oroojlooy and Hajinezhad, 2023; Wong *et al.*, 2023] offers a powerful framework for controlling large-scale systems by enabling multiple agents to learn collectively while interacting within a shared, dynamic environment. In MARL, agents seek to optimize their policies based on accumulated experience, derived from the history of their interactions with both the environment and other agents. A central objective of MARL research is to develop algorithms that achieve effective learning with minimal experience, thereby improving sample efficiency.

Despite its promise, MARL presents several fundamental challenges, including the need for coordination among

agents, non-stationarity induced by concurrently evolving policies, and scalability to systems with many agents. To address these challenges, advanced MARL methods incorporate a range of techniques such as decentralized or partially centralized training, explicit communication mechanisms, and hierarchical structures that facilitate efficient multi-agent coordination. Ongoing theoretical developments and practical successes highlight the versatility of MARL across a broad spectrum of applications, including robotics [Orr and Dutta, 2023], autonomous driving [Yadav *et al.*, 2023; Schmidt *et al.*, 2022; Althamary *et al.*, 2019], and telecommunications [Li *et al.*, 2022b; Feriani and Hossain, 2021].



Figure 1: The strategic sacrifice tactics found by MACTAS for the 3s5z_vs_3s6z map from the SMAC benchmark, on which MACTAS outperforms the baselines significantly. The agent at the top of the figure (“Local Player”) lures the opponents away and sacrifices its own life to enable the remaining agents to gain a strategic advantage and win the episode.

Two of the most actively studied directions in MARL are action-value function decomposition methods [Wang *et al.*, 2021; Liu *et al.*, 2023b], which allocate a shared team reward according to individual agent contributions, and inter-agent communication mechanisms [Liu *et al.*, 2023a; Guo *et al.*, 2023], which enable coordination through information exchange. Many of the most challenging multi-agent environments are only partially observable, often restricting

*Equal contribution.

agents' perceptions to their local neighborhoods. In such settings, successful task completion critically depends on effective coordination, which in turn typically requires some form of communication. In our proposed architecture, communication is integrated directly into the action–value function decomposition itself.

The dominant framework for cooperative MARL is *Centralized Training and Decentralized Execution* (CTDE), wherein the learning algorithm has access to the global state during training, while each agent relies solely on its local observations at execution time. We contend that this paradigm is inadequate for many complex MARL problems. In practice, reliable inter-agent communication is often feasible—for example, via wireless networks—and can significantly enhance coordination. Motivated by this observation, we introduce a communication mechanism based on self-attention: The latent state of each agent is updated based on other agents' states, similar to how word embeddings are updated based on other words in the Transformer encoder [Vaswani *et al.*, 2017]. By leveraging self-attention, the proposed architecture requires only a constant number of shared parameters, along with agent-specific embeddings. Furthermore, it can be efficiently implemented using standard Transformer encoder layers, making it both scalable and practical.

Although self-attention has been employed in different contexts in MARL before, including communication, this is the first successful approach to using self-attention on its own as a communication tool in MARL, without the need for graph-structure learning or global state reconstruction. Moreover, our method can be combined with an arbitrary action–value decomposition. None of the previous works has applied self-attention directly as a communication protocol. Our work fills this gap. It is the first algorithm showing that self-attention on agent internal states is sufficient for effective and reliable communication without the need for explicit teammate modeling or message preparation mechanisms.

The contribution of this paper includes:

- We introduce Multi-Agent Communication via Transformer on Agents' States (MACTAS) for inter-agent communication in MARL based on a self-attention mechanism applied directly to internal state embeddings of agents. MACTAS is the first self-attention-based communication mechanism with the number of trainable parameters independent of the number of agents, which makes it scalable to large systems. Moreover, it can be combined with any action–value function mixing architecture.
- We verify experimentally MACTAS in combination with the most popular decomposition methods on challenging maps from SMACv2, showing results better than current state-of-the-art algorithms in most cases. We also perform experiments on SMAC, Level-based Foraging, and Hallway, proving that MACTAS is more reliable in a diverse set of scenarios.

Our approach outperforms state-of-the-art communication algorithms (including a method that uses self-attention and global state reconstruction) in combination with common mixers. Moreover, our method proves robust on a diverse set

of tasks, while each baseline fails on some relatively simple task (like Hallway or the 2c_vs_64zg SMAC map). Our algorithm can learn sophisticated tactics, such as sacrificing one agent to win the entire battle (as shown in Figure 1). A detailed study of the tactics found by our method is presented in Appendix E.

2 Related Work

Single-agent reinforcement learning (SARL) [Sutton and Barto, 2018] studies trial-and-error learning for sequential decision-making under uncertainty. Multi-agent reinforcement learning (MARL) [Ning and Xie, 2024] generalizes this framework to settings in which multiple agents simultaneously interact with and influence a shared, dynamic environment. MARL encompasses a wide range of problem formulations, varying along dimensions such as synchronous versus asynchronous decision-making, cooperative versus competitive objectives, and differing information structures. In this work, we restrict our attention to the synchronous, fully cooperative setting, where all agents share a common reward signal at each time step.

A major limitation of the CTDE framework is the exponential growth of the joint action–value function with the number of agents [Kraemer and Banerjee, 2016]. As a result, action–value function decomposition has emerged as a central challenge in MARL. Decomposition-based architectures typically assign each agent a local module that processes its observations and previous actions to produce an individual contribution to the global value. An agent's optimal action is then determined by maximizing its contribution to the joint value estimate.

Several decomposition approaches have been proposed in the literature. Value Decomposition Networks (VDN) [Sunehag *et al.*, 2018] aggregate agent contributions through simple summation, while QMIX [Rashid *et al.*, 2018] employs a mixing network that computes a weighted sum with non-negative weights to preserve monotonicity. Weighted QMIX [Rashid *et al.*, 2020] further refines this approach by assigning special weights to optimal joint actions during training. QTRAN [Son *et al.*, 2019] introduces an auxiliary module that incorporates the joint action to correct the decomposed value. Attention mechanisms are leveraged in Qatten [Yang *et al.*, 2020] to construct a more flexible mixing network. Additional extensions include CDS [Li *et al.*, 2021], which adjusts agent exploration through the mixing network; DVD [Li *et al.*, 2022a], which incorporates agents' internal states into value aggregation; SHAQ [Wang *et al.*, 2022], which augments the mixing network using principles from Shapley value theory; QPLEX [Wang *et al.*, 2021], which introduces a duplex dueling architecture over agent contributions; and NA²Q [Liu *et al.*, 2023b], which adopts a similar duplex dueling strategy enhanced with attention mechanisms.

Another fundamental problem in cooperative MARL is the coordination of agents' activities, which requires a communication protocol. A number of solutions have been proposed for this purpose: CommNet [Sukhbaatar *et al.*, 2016] introduces differentiable communication by aggregating a learned broadcast vector from each agent, TarMAC [Das *et al.*, 2019]

uses signature-based soft attention to direct agent communication towards recipients, NDQ [Wang *et al.*, 2019] applies two forms of regularization – mutual information maximization and message entropy minimization to optimize message content, GA-Comm [Liu *et al.*, 2020] uses two-stage attention mechanism to limit number of messages exchanged between agents, IS [Kim *et al.*, 2021] encodes trajectory of future actions for each agent and shares them with others, DHCG [Liu *et al.*, 2023a] learns a dependency graph between agents and uses it to limit the number of communication edges, TEM [Guo *et al.*, 2023] uses a Transformer to simulate communication resembling email exchange, where agents only directly communicate with teammates nearby, but can forward messages from one to another, ExpoComm [Li *et al.*, 2025] utilizes exponential graphs to design the communication topology. Also, in MAIC [Yuan *et al.*, 2022] agents explicitly model their teammates and use it to bias their value function, MASIA [Guan *et al.*, 2022] uses attention-based communication architecture with a decoder module to reconstruct the global state, CommFormer [Hu *et al.*, 2024] uses the attention encoder and decoder architecture combined with learning a communication graph, having the number of parameters independent of the number of agents.

In addition, there are solutions in which the agents communicate in natural language, including: TWOSOME [Tan *et al.*, 2024] which uses a large language model (LLM) to evaluate the probabilities of joint action and applies LoRa for efficient PPO training, and Verco [Li *et al.*, 2024] which separates the output of the LLM into communication and actions, allowing LLM agents to exchange interpretable verbal messages.

Attention and Transformer architectures have been applied in MARL algorithms, such as in Qatten and NA²Q mixing networks, or in communication mechanisms like GA-Comm, TEM, CommFormer, and MASIA. However, our approach is conceptually different: We apply the attention mechanism directly to generate the agents’ messages, without additional graph-structure learning (as in CommFormer) or decoding the global state (as in MASIA). Our proposed use of attention makes the number of trainable parameters independent of the number of agents (which enables deployment at scale), unlike in MASIA. Moreover, our method can be combined with any mixing architecture, unlike CommFormer. We consider communication methods that can be coupled with an arbitrary action-value decomposition method. We also allow agents to send messages based only on their local information (current observation, historical observations, and historical actions). In this framework, MAIC has achieved the best results so far. MASIA is a communication protocol that uses self-attention. Therefore, in the experimental study, we compare our proposed MACTAS to both MAIC and MASIA.

3 Method

In this section, we formalize the problem statement, present the details of applying self-attention in MACTAS, and discuss its distributed deployment.

Problem definition. In this paper, we discuss the problem of MARL using the formalism of a cooperative Decentralized Partially Observable Markov Decision Process (Dec-

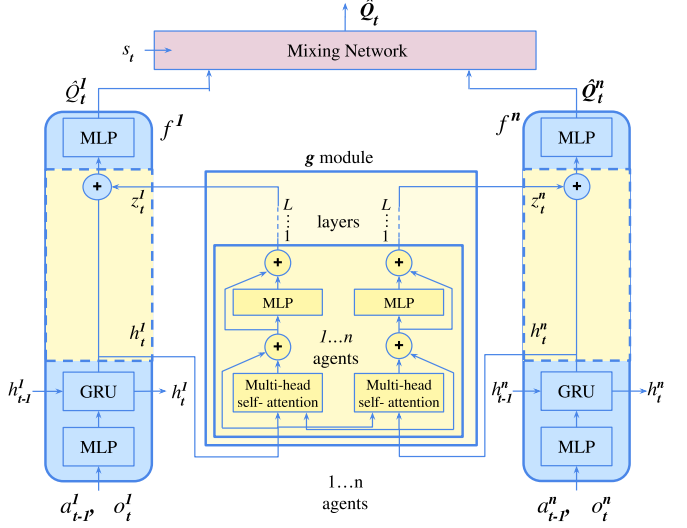


Figure 2: The proposed MACTAS architecture.

POMDP) with communication. Dec-POMDP is defined by a tuple $\langle \mathbb{N}, \mathbb{S}, \mathbb{A}, \mathcal{R}, \mathcal{P}, \Omega, \mathcal{O}, \gamma \rangle$, where $\mathbb{N} = \{1, \dots, n\}$ represents the team of agents, \mathbb{S} is the global environmental state space, $\mathbb{A} = \mathbb{A}^1 \times \dots \times \mathbb{A}^n$ is the joint action space, $\mathcal{R} : \mathbb{S} \times \mathbb{A} \times \mathbb{S} \rightarrow \mathbb{R}$ is the reward function, $\mathcal{P} : \mathbb{S} \times \mathbb{A} \rightarrow P(\mathbb{S})$ is the state transition probability function, $\Omega = \Omega^1 \times \dots \times \Omega^n$ is the joint observation space, $\mathcal{O} : \mathbb{N} \times \mathbb{S} \rightarrow \Omega$ is the observation function and $\gamma \in [0, 1]$ is the discount factor. At time $t = 1, 2, \dots$ the i -th agent makes an observation, $o_t^i = \mathcal{O}(i, s_t), o_t^i \in \Omega^i$, of the environment state $s_t \in \mathbb{S}$. Agents may exchange messages through a channel that generally refines them with some processing.

We define a set of representations $\mathcal{J} = \mathcal{J}^1 \times \dots \times \mathcal{J}^n$. Each agent at timestep t maintains a representation, $\mathcal{I}_t^i \in \mathcal{J}^i$, of observations it has made, messages it has received, and actions it has taken. Based on thereof and a policy, $\pi^i : \mathcal{J}^i \rightarrow \mathbb{A}^i$, the agent performs an action, $a_t^i \in \mathbb{A}^i$, $a_t^i \sim \pi^i(\cdot | \mathcal{I}_t^i)$. The team action $a_t = [(a_t^1), \dots, (a_t^n)]$ impacts the next environment state $s_{t+1} \sim \mathcal{P}(\cdot | s_t, a_t)$ and the reward $r_t = \mathcal{R}(s_t, a_t, s_{t+1})$ is given collectively to all agents.

The goal of the agents’ learning is to optimize their team policy $\pi = [\pi^1, \dots, \pi^n]$ to expect in each environment state s the highest sum of discounted rewards:

$$\mathcal{V}^\pi(s) = \mathbb{E} \left(\sum_{i \geq 0} \gamma^i r_{t+i} \mid s_t = s, \text{policy in use} = \pi \right).$$

The goal of this paper is to establish the message exchange protocol that supports the above learning goal.

Self-attention as communication protocol. Suppose at time step t , each agent i maintains a latent state $h_t^i \in \mathbb{R}^{n_h}$ (we use the horizontal vector notation) derived from its observations up to that point. To select an optimal action, an agent should incorporate information about other agents’ states. To facilitate such information sharing, we employ a self-attention mechanism [Vaswani *et al.*, 2017]. Specifically, let $M^k, M^q, M^v \in \mathbb{R}^{n_h \times n_h}$ denote learnable projec-

tion matrices. Agent i updates its representation by aggregating the states of all agents, where the contribution of agent j is given by $\alpha_t^{i,j} h_t^j M^v$. The attention weight $\alpha_t^{i,j}$ is proportional to $\exp\left(h_t^i M^q (h_t^j M^k)^T / \sqrt{n^h}\right)$, and is normalized such that $\sum_j \alpha_t^{i,j} = 1$. This weighting reflects the relevance of agent j 's state to agent i at time t .

The Transformer encoder introduced in [Vaswani *et al.*, 2017] augments self-attention with several additional components. These include (i) multi-head attention, which allows different subspaces of the state representations to be attended to in parallel; (ii) a feedforward MLP applied to the attention outputs; (iii) layer normalization applied after residual updates; and (iv) stacking multiple such blocks to form deep architectures. We adopt this Transformer encoder structure to enable effective and flexible information exchange among agents.

MACTAS. Our proposed Multi-Agent Communication via Transformer on Agents States (MACTAS) architecture is presented in Fig. 2. It is built on a decomposition of the action-value function. Each such decomposition includes the input modules assigned to the agents (f^i assigned to the i -th agent for $i = 1, \dots, n$ in Figure 2). These modules are fed with previous actions of these agents, a_{t-1}^i , and their current observations, o_t^i . They produce agents' contributions, \hat{Q}_t^i , to future discounted rewards and perhaps some other vectors [Li *et al.*, 2022a]. The outputs of the f^i modules are fed to the mixing network that produces the value of the action-value function, \hat{Q}_t . The input module f^i usually comprises a feedforward part, denoted by MLP in Figure 2, a recurrent part, denoted by GRU, and the output feedforward part, again denoted by MLP.

Intuitively, we understand the f^i module as the “awareness” of the i -th agent. Based on what the agent is aware of, it determines its contribution to future discounted rewards, depending on the action it currently takes. In order to give a global view on the current state to the agent's “awareness”, we introduce a communication mechanism. We divide the f^i module after its recurrent part and feed its state $h_t^i \in \mathbb{R}^{n_h}$ to the module g , where the states of “awareness” of the agents are confronted. As a result, the g module produces increments, $z_t^i \in \mathbb{R}^{n_h}$. The sum $z_t^i + h_t^i$ is then passed to the second MLP part of the f^i module.

Consequently, the “awareness” of each agent is based not only on its observations and previous actions, but also on observations and previous actions of all other agents.

The minimal requirement for the g module is as follows:

1. It is fed with n vectors and produces n vectors, both of size $\dim(h_t^i)$. The i -th input vector corresponds to the i -th output vector.
2. It is a layered structure and the layers include self-attention [Vaswani *et al.*, 2017].

Introducing g that satisfies the above requirements in their basic form is enough to outperform MARL without communication by a large margin. However, what follows from our experiments is that usually the best performing form of

the g module is a stack of Transformer (encoder) modules [Vaswani *et al.*, 2017], with the following settings:

1. There are no positional embeddings. The agents' embeddings are fed to f^i instead.
2. There is no masking.
3. We use a separate Adam optimizer [Kingma and Ba, 2017] for the Transformer parameters; the rest of the architecture is trained with its originally proposed optimizer (typically RMSProp [Tieleman and Hinton, 2012]).
4. The weights of the output layer of the top Transformer module are initialized with zeros. Therefore, initially, this module does not affect the agents' state of “awareness”.

A good performance of the Transformer in this role is expected. This architecture has been specifically optimized to transform a set of embeddings into another set of the same size, which is exactly what we require in the g module.

Distributed deployment. The basic approach to implement a multi-agent system with our proposed MACTAS module is to set up the Intermediate Processing Unit (IPU) on which the module is run. At each time instant, all n agents transmit their internal states h_t^i to the IPU. Then, the Transformer layers process all the input vectors and transmit the increments z_t^i back to the agents. The number of operations necessary to process the Transformer modules is $O(n^2)$. However, they are very efficiently parallelizable. The total size of all the transmissions is $O(n)$, specifically, equal to $2n \dim(h_t^i)$.

Usually in multi-agent systems, reducing the communication capacity to $O(n)$ and offloading the communication processing burden to the IPU is very convenient. In these systems, the agents are naturally connected through a network and their computational capacity is limited (e.g., they are mobile and battery-powered), contrary to that of the network infrastructure. Still, these are the agents that need to take on the processing of their observations and control.

In most inter-agent communication protocols, including MAIC [Yuan *et al.*, 2022], all pairs of agents need to be able to communicate, which translates into $O(n^2)$ messages. Technically, the parts of the agents that communicate with others could be moved to an IPU. Communication through the IPU would require $O(n)$ messages from the agents to the IPU and back. Still, natural parallelization of MACTAS is its noticeable advantage.

A distributed implementation of a multi-agent system with our proposed module is also possible. Then, each agent needs to take on the part of processing that consists of refining h_t^i and results in z_t^i . That requires exchanging messages with other agents as many times as there are Transformer layers in MACTAS, each time with $O(n)$ messages; $O(n^2)$ for all agents. In training, the agents need to aggregate increments in their shared weights.

In a distributed implementation, some agents may be out of reach of others and not exchange information with them. That only means that self-attention in MACTAS is forced to

Scenario	Stacked encoders	FFN dimension
all SMACv2 maps	3	512
2c_vs_64zg	2	512
5m_vs_6m, 27m_vs_30m	1	128
MMM2	3	256
6h_vs_8z, 3s5z_vs_3s6z	3	512
LBF and Hallway	1	32

Table 1: MACTAS shape for each scenario.

assign zero weight to unavailable transmissions from those unheard agents.

4 Experiments

In this section, we present the results of our proposed MACTAS communication protocol in the StarCraft Multi-Agent Challenge environments (SMACv2 [Ellis *et al.*, 2023] and SMAC [Samvelyan *et al.*, 2019]). We compare it with the state-of-the-art MAIC [Yuan *et al.*, 2022] and MASIA [Guan *et al.*, 2022], in combination with 3 mixer algorithms: QMIX, QPLEX, and VDN, on 9 SMACv2 maps and in combination with QMIX on 6 SMAC maps. We also present results in combination with QMIX on Level-based Foraging [Papoudakis *et al.*, 2021] and Hallway [Wang *et al.*, 2019].

4.1 StarCraft Multi-Agent Challenge

The StarCraft Multi-Agent Challenge (SMAC and SMACv2) is a micromanagement benchmark where two opposing teams face each other in different scenarios (maps), with one team controlled by the RL agent and the other by a built-in algorithm. Maps differ by difficulty, mainly due to an imbalance in the number of controlled units. For our experiments, we selected 9 SMACv2 maps (3 maps with 5 against 5 agents, 3 maps with 10 against 11 agents, and 3 maps with 20 against 23 agents) and 6 maps from SMAC scenarios, which are widely benchmarked in the MARL community (2c_vs_64zg, 5m_vs_6m, 27m_vs_30m, MMM2, 6h_vs_8z, 3s5z_vs_3s6z), the first 2 being hard and the latter 4 super-hard.

On SMAC, every map provides the opportunity to find a unique winning strategy. The agent requires learning basic skills, such as navigating the battlefield, managing health and shield, or focusing fire. All considered scenarios are imbalanced in favor of the enemies; therefore, simple strategies are insufficient to win the episode. Popular observed winning policies include crossing the obstacle on 2c_vs_64zg, flanking on 27m_vs_30m, 'kiting' on 6h_vs_8z, 'hit and run' on 3s5z_vs_3s6z [Samvelyan *et al.*, 2019]. However, the standard version of SMAC is easily solved by quite simple algorithms. Thus, we borrow the setup from MAIC [Yuan *et al.*, 2022], in which the episode limits for maps have been shortened, making the benchmark challenging for newer algorithms.

SMACv2 [Ellis *et al.*, 2023] is a newer iteration of SMAC, which introduces new maps focused on scenario randomization. Each of the new maps defines the race (the same for both teams) and the number of units in each team, while the exact types and starting positions are randomized according

to the configuration. We use the default configuration for each scenario recommended in the SMACv2 repository.

4.2 Level-based Foraging and Hallway

We also compare MACTAS with baselines on two toy problems: Level-based Foraging (LBF) and Hallway. The first benchmark is a grid-world (we use 10×10) with agents and food. Each agent and food has a level, which is randomly assigned (in our experiments, the agent's level is at most 3 and the food's level is at most 2). An agent can move in four directions, perform "none" action, and load food. To collect the food, a group of agents must collectively perform the load action, and the sum of their levels must be at least as great as the food's level. Agents obtain a reward for eating food, and their goal is to maximize the return in the fixed horizon (we use 50 steps). The maximal return is normalized to 1. Moreover, each agent can observe only the fixed radius around them (we use radius 2).

Hallway is a sparse-reward coordination task with k agents. Agent i has a corridor of length m_i , is initialized in this corridor, and can move right (apart from the right end of the corridor) and left. There is a special common state g to which each agent can move, taking a step to the left from the left end of their corridor. The agents' goal is to move simultaneously to the state g . We use $k = 3, m_1 = 2, m_2 = 6, m_3 = 10$.

4.3 Experimental setting

We borrow the basic settings from NA²Q [Liu *et al.*, 2023b] and extend their code with implementations of MACTAS, MAIC, and MASIA. The algorithms are trained using the Double Q-Learning [Hasselt *et al.*, 2016] algorithm. Detailed hyperparameters are available in the Appendix. Each experiment is run for a fixed number of training episode steps – 2.0 million for LBF and Hallway, 2.5 million for 2c_vs_64zg, 5m_vs_6m, MMM2, 27m_vs_30m SMAC environments and 7.5 million for 6h_vs_8z, 3s5z_vs_3s6z and all SMACv2 environments, interleaved with test episodes every 10000 steps. Each experiment is repeated for seeds 1, ..., 5. We report the average percentage of wins in test games, along with the standard deviations, in Table 2, learning curves for the zerg race in Figure 3, and the remaining learning curves in the Appendix. For MAIC and MASIA communication, we employ the same hyperparameters as those used in the original papers.

MACTAS hyperparameters. We notice that MACTAS is sensitive to communication hyperparameters depending on the scenario setup. The parameters are the number of stacked Transformer encoders and the dimension of their positional feedforward network block. We theorize that the depth and width of the communication channel create a trade-off between the ability to learn a complex joint policy (e.g., kiting, hit-and-run) and the time it takes to learn an effective policy. We perform a hyperparameter search, for which detailed results are included in the Appendix, and use the values presented in Table 1. We use $d_{model} = 64$ in the Transformer architecture (equal to the RNN size).

Mixer compatibility. MACTAS, MAIC, and MASIA are agnostic to the value function decomposition algorithm, so

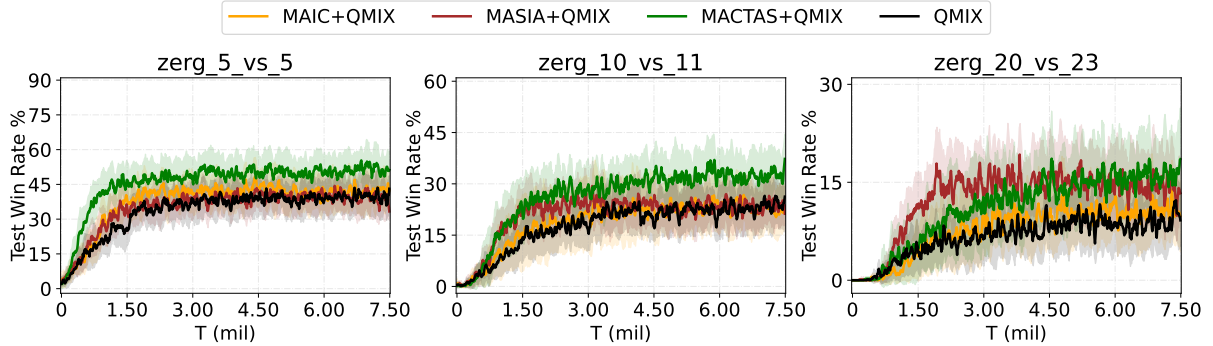


Figure 3: Training curves for the zerg race on the SMACv2 benchmark with the QMIX mixer.

we compare all algorithms in combination with commonly used mixers: VDN, QMIX, and QPLEX. Each combination, named **MACTAS+VDN**, **MAIC+QPLEX**, etc., is tested across all SMACv2 maps and compared separately to provide a fair comparison and isolate the effect of the mixer on the achieved results. We conduct additional experiments on SMAC, LBF, and Hallway with the QMIX mixer, as it is the default one for MAIC and MASIA.

4.4 Results

The basic results are presented in Table 2.

SMACv2. We compare MACTAS with MAIC, MASIA, and the bare mixer on 9 maps and 3 different mixers. Our method achieves the best results on most maps. Moreover, MASIA fails to achieve a positive score for some scenarios, while MACTAS does not degenerate in such a manner. MAIC+QPLEX results in NaN errors in some runs.

SMAC. We compare MACTAS with MAIC and MASIA on 6 maps, 2 hard and 4 super-hard. Two of the super-hard maps (6h_vs_8z, 3s5z_vs_3s6z) are particularly challenging and thus require more training steps and a longer epsilon annealing period. MACTAS excels on these two maps; however, it is not the best method on three simpler maps. Moreover, we observe that on these simpler maps, a smaller Transformer architecture (fewer layers and a smaller feed-forward network) is usually required to obtain good results. This shows a trade-off between learning complex strategies for the most challenging scenarios and rapid learning of simpler strategies for simpler tasks. We also observe that MASIA fails to solve the simplest 2c_vs_64zg task, on which other methods achieve above 95% of the win rate.

LBF and Hallway. We observe that all methods solve the LBF task (above 90% test mean reward). On the Hallway benchmark, MAIC and the bare mixer fail (below the 5% test battle win rate), while MACTAS and MASIA achieve the 100% test battle win rate.

4.5 Ablations

We observe that the performance of MACTAS is not as outstanding on the SMAC benchmark as on the SMACv2. We hypothesize that the randomization introduced in SMACv2 requires finding more diverse policies and thus allows for

showing the strength of MACTAS. To verify this hypothesis, we conduct an experiment in which, for a given seed, we fix the SMACv2 scenario and train on it MACTAS and MASIA. We observe that when the randomization is turned off in such a manner, MASIA can perform on a par with MACTAS (after 2.5 million training steps on protoss_5_vs_5 MACTAS achieves $96.3 \pm 6.8\%$ of the battle win rate and MASIA achieves $90.0 \pm 11.1\%$, on zerg_5_vs_5 MACTAS achieves $96.3 \pm 4.1\%$ and MASIA achieves $90.6 \pm 10.4\%$, training curves are available in the Appendix).

We notice that the Transformer module includes residual connections. The question is whether the residual connection around it (the arrow between GRU and “+” in Fig. 2) is helpful indeed. Thus, we compare the version of MACTAS without this connection to the default one. We observe that the absence of this residual connection hampers performance on more complex scenarios (final performance on 3s5z_vs_3s6z without this residual connection is $59.4 \pm 33.2\%$, and with the connection is $88.8 \pm 4.2\%$; an extended comparison is available in the Appendix).

We compare different numbers of stacked Transformer layers for SMACv2 and conduct a broad hyperparameter search for the number of layers and the feedforward network size for SMAC in the Appendix (as we observe that MACTAS requires a dedicated architecture choice in these tasks). We also test several feedforward network sizes for LBF and Hallway in the Appendix. We observe that the architecture choice is important for the SMAC, LBF, and Hallway benchmarks, but the optimal architecture is not unique. Moreover, in almost all the studied cases, the versions of MACTAS outperform the bare mixer (i.e., communication turned off).

4.6 Robustness study

Previous experiments were performed in perfect connectivity conditions. In a distributed implementation, where each agent runs on separate hardware, communication must be performed over networks with potential disruptions and connectivity loss. We validate MACTAS in these conditions by simulating network volatility – the connectivity state $c_{i,j}$ between agents i and j at time t is updated according to:

$$c_{i,j}^{(t)} = \begin{cases} X \sim \text{Bernoulli}(p) & \text{with probability } q \\ c_{i,j}^{(t-1)} & \text{with probability } 1 - q \end{cases} \quad (1)$$

Map_name	(ours)	MACTAS	MASIA	MAIC	Bare mixer
↪ Mixer	MACTAS				
zerg_5_vs_5					
↪ QMIX	50.0±6.6	29.4±5.2	40.6±11.5	45.0±11.8	
↪ VDN	57.5±11.8	35.0±7.1	33.8±9.2	33.8±4.6	
↪ QPLEX	56.3±7.7	36.9±12.2	47.5±7.1	48.1±11.2	
zerg_10_vs_11					
↪ QMIX	34.4±9.9	18.8±4.9	26.3±10.5	25.6±11.8	
↪ VDN	31.3±8.3	25.0±13.4	16.3±5.1	13.1±6.8	
↪ QPLEX	36.3±10.5	1.3±1.7	19.4±18.0*	19.4±2.6	
zerg_20_vs_23					
↪ QMIX	16.9±6.5	16.9±4.7	10.0±4.1	10.0±3.4	
↪ VDN	13.8±3.6	8.8±6.0	8.8±6.0	9.4±4.9	
↪ QPLEX	21.9±4.4	0.0±0.0	13.8±13.0*	16.3±5.6	
terran_5_vs_5					
↪ QMIX	71.9±3.1	0.0±0.0	66.9±7.2	66.9±2.8	
↪ VDN	61.3±14.1	0.0±0.0	70.0±13.5	58.1±9.5	
↪ QPLEX	67.5±18.2	0.0±0.0	80.0±6.5	68.1±12.0	
terran_10_vs_11					
↪ QMIX	39.4±11.2	40.0±13.0	41.3±9.7	36.9±5.1	
↪ VDN	43.8±4.9	20.6±9.8	32.5±8.1	31.3±3.1	
↪ QPLEX	50.6±11.4	9.4±5.8	16.3±22.3*	45.6±9.8	
terran_20_vs_23					
↪ QMIX	12.5±8.0	15.0±6.8	10.0±4.1	8.8±9.5	
↪ VDN	8.1±4.7	7.5±6.8	4.4±5.2	2.5±1.4	
↪ QPLEX	16.3±5.1	0.0±0.0	8.1±11.6*	11.9±10.5	
protoss_5_vs_5					
↪ QMIX	70.6±5.2	58.8±11.8	61.9±9.2	61.3±7.5	
↪ VDN	73.8±15.2	40.6±12.3	68.1±7.1	61.3±13.2	
↪ QPLEX	70.0±7.8	56.9±13.1	70.0±6.5	60.6±11.4	
protoss_10_vs_11					
↪ QMIX	42.5±11.2	25.6±7.8	33.8±14.9	27.5±14.0	
↪ VDN	37.5±11.3	18.1±8.7	24.4±3.4	25.6±5.1	
↪ QPLEX	45.0±11.4	21.3±8.4	40.0±8.4	26.9±9.3	
protoss_20_vs_23					
↪ QMIX	15.0±10.7	13.1±6.0	15.0±3.4	10.6±6.8	
↪ VDN	9.4±9.6	6.3±2.2	5.0±2.8	2.5±1.4	
↪ QPLEX	16.9±7.8	3.8±8.4	11.9±10.2	5.6±3.4	
2c_vs_64zg					
↪ QMIX	99.4±1.4	17.5±28.8	98.1±2.8	98.8±1.7	
5m_vs_6m					
↪ QMIX	69.4±11.6	78.1±7.0	76.9±11.6	65.0±14.9	
27m_vs_30m					
↪ QMIX	78.8±12.6	93.1±8.7	87.5±7.0	75.6±11.8	
MMM2					
↪ QMIX	77.5±10.5	90.0±1.4	93.8±3.1	69.4±39.1	
6h_vs_8z					
↪ QMIX	86.9±6.8	0.0±0.0	56.9±20.1	20.0±30.4	
3s5z_vs_3s6z					
↪ QMIX	88.8±4.2	13.8±27.3	71.9±9.6	51.9±23.7	
hallway_3a_1g					
↪ QMIX	100.0±0.0	100.0±0.0	0.0±0.0	1.8±2.1	
lbf-4-2					
↪ QMIX	93.8±2.6	91.6±4.3	95.7±1.6	91.8±2.4	

Table 2: Final scores (in percent) across maps from SMACv2, SMAC, Hallway (win rate) & LBF (mean reward), for different combinations of mixers and communication algorithms. **Bold** highlights the statistically important best of the row. Colors are interpolated between white and green, based on the mean scaled between 0.0 and the max of each row. * indicates NaN errors for some runs, see Appendix A.2

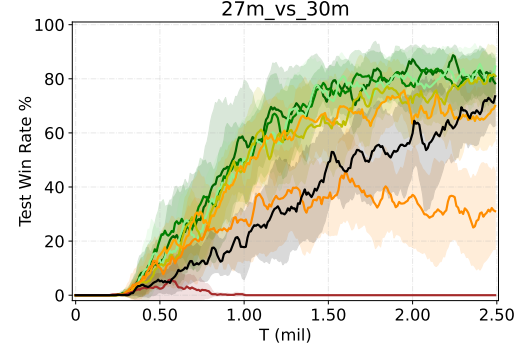
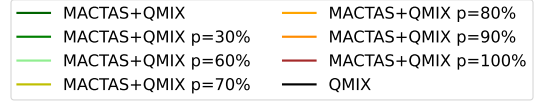


Figure 4: Connectivity disruption simulation results at different p values.

where q is the state-change probability (we use 10%) and p is the probability of a functional connection (% disruption).

Figure 4 presents the results of the study. Communication via the attention matrix is masked according to the above equation. Agents are trained according to the standard procedure, but are evaluated with a communication disturbance. No other changes are made to the training process or state definition; i.e., the masking matrix is not stored in the state and is not provided as an input to the model during inference or training. Weight updates remain unaware of any communication disruptions, making the learning conditions highly adversarial. MACTAS proofs immune to connectivity disruption up to $p = 60\%$, while maintaining relatively strong performance up to $p = 80\%$, showing a noticeable decline towards $p = 100\%$ where self-attention communication starts to disturb the learning process due to the distribution shift between training and execution. Further reference can be found in Appendix A.3.

5 Discussion and conclusions

In this paper, we introduce MACTAS – a novel communication method for multi-agent reinforcement learning. We leverage the Transformer encoder architecture to ensure state-of-the-art performance and robust communication in heavy adversarial conditions. Moreover, it requires a fixed number of parameters independent of the number of agents, making it scalable to large systems. It can be easily switched in any multi-agent action-value function architecture. We evaluated our proposed module on SMACv2 and SMAC, arguably the most challenging MARL benchmarks, as well as two toy problems: LBF and Hallway. The experimental results show that MACTAS outperforms the baselines across most scenarios with all the tested mixers and demonstrates robustness across all tested environments.

The modular nature of MACTAS is its great advantage. There are widespread variants of the Transformer code optimized for different machines, such as PyTorch [Paszke *et al.*, 2019]. This makes the implementation and deployment

of MACTAS in a given MARL system straightforward.

Limitations. The performance of MACTAS on SMAC, LBF, and Hallway is moderately sensitive to the shape of the communication module defined by the number of layers and the size of the hidden layer of the MLP contained there, requiring searching for its best setting in additional runs. This slightly slows down the deployment of MACTAS.

Ethical Statement

There are no ethical issues.

Acknowledgments

We gratefully acknowledge the Polish high-performance computing infrastructure PLGrid (HPC Center: ACK Cyfronet AGH) for providing computer facilities and support within the computational grant no. PLG/2025/018560 and no. PLG/2025/017992. We thank the University of Warsaw for providing access to the computing infrastructure.

References

[Althamary *et al.*, 2019] Ibrahim Althamary, Chih-Wei Huang, and Phone Lin. A survey on multi-agent reinforcement learning methods for vehicular networks. In *International Wireless Communications & Mobile Computing Conference (IWCMC)*, pages 1154–1159, 2019.

[Das *et al.*, 2019] Abhishek Das, Théophile Gervet, Joshua Romoff, Dhruv Batra, Devi Parikh, Mike Rabbat, and Joelle Pineau. TarMAC: Targeted multi-agent communication. In *International Conference on Machine Learning (ICML)*, pages 1538–1546, 2019.

[Du and Ding, 2021] Wei Du and Shifei Ding. A survey on multi-agent deep reinforcement learning: from the perspective of challenges and applications. *Artificial Intelligence Review*, 54:3215–3238, 2021.

[Ellis *et al.*, 2023] Benjamin Ellis, Jonathan Cook, Skander Moalla, Mikayel Samvelyan, Mingfei Sun, Anuj Mahajan, Jakob Foerster, and Shimon Whiteson. Smacv2: An improved benchmark for cooperative multi-agent reinforcement learning. In *Advances in Neural Information Processing Systems (NeurIPS)*, volume 36, pages 37567–37593, 2023.

[Feriani and Hossain, 2021] Amal Feriani and Ekram Hossain. Single and multi-agent deep reinforcement learning for ai-enabled wireless networks: A tutorial. *IEEE Communications Surveys & Tutorials*, 23(2):1226–1252, 2021.

[Guan *et al.*, 2022] Cong Guan, Feng Chen, Lei Yuan, Chenghe Wang, Hao Yin, Zongzhang Zhang, and Yang Yu. Efficient multi-agent communication via self-supervised information aggregation. In *Advances in Neural Information Processing Systems (NeurIPS)*, volume 35, pages 1020–1033, 2022.

[Guo *et al.*, 2023] Xudong Guo, Daming Shi, and Wenhui Fan. Scalable communication for multi-agent reinforcement learning via transformer-based email mechanism. In *International Joint Conference on Artificial Intelligence (IJCAI)*, 2023. arXiv:2301.01919.

[Hasselt *et al.*, 2016] Hado van Hasselt, Arthur Guez, and David Silver. Deep reinforcement learning with double q-learning. In *AAAI Conference on Artificial Intelligence (AAAI)*, page 2094–2100, 2016.

[Hu *et al.*, 2024] Shengchao Hu, Li Shen, Ya Zhang, and Dacheng Tao. Learning multi-agent communication from graph modeling perspective. In *International Conference on Representation Learning*, volume 2024, pages 12963–12978, 2024.

[Kim *et al.*, 2021] Woojun Kim, Jongeui Park, and Youngchul Sung. Communication in multi-agent reinforcement learning: Intention sharing. In *International Conference on Learning Representations (ICLR)*, 2021.

[Kingma and Ba, 2017] Diederik P. Kingma and Jimmy Ba. Adam: A method for stochastic optimization, 2017. arXiv:1412.6980.

[Kraemer and Banerjee, 2016] Landon Kraemer and Bikramjit Banerjee. Multi-agent reinforcement learning as a rehearsal for decentralized planning. *Neurocomputing*, 190:82–94, 2016.

[Li *et al.*, 2021] Chenghao Li, Tonghan Wang, Chengjie Wu, Qianchuan Zhao, Jun Yang, and Chongjie Zhang. Celebrating diversity in shared multi-agent reinforcement learning. In *Advances in Neural Information Processing Systems (NeurIPS)*, volume 34, pages 3991–4002, 2021.

[Li *et al.*, 2022a] Jiahui Li, Kun Kuang, Baoxiang Wang, Furu Liu, Long Chen, Changjie Fan, Fei Wu, and Jun Xiao. Deconfounded value decomposition for multi-agent reinforcement learning. In *International Conference on Machine Learning (ICML)*, volume 162, pages 12843–12856, 2022.

[Li *et al.*, 2022b] Tianxu Li, Kun Zhu, Nguyen Cong Luong, Dusit Niyato, Qihui Wu, Yang Zhang, and Bing Chen. Applications of multi-agent reinforcement learning in future internet: A comprehensive survey. *IEEE Communications Surveys & Tutorials*, 24(2):1240–1279, 2022.

[Li *et al.*, 2024] Dapeng Li, Hang Dong, Lu Wang, Bo Qiao, Si Qin, Qingwei Lin, Dongmei Zhang, Qi Zhang, Zhiwei Xu, Bin Zhang, and Guoliang Fan. Verco: Learning coordinated verbal communication for multi-agent reinforcement learning, 2024. arXiv:2404.17780.

[Li *et al.*, 2025] Xinran Li, Xiaolu Wang, Chenjia Bai, and Jun Zhang. Exponential topology-enabled scalable communication in multi-agent reinforcement learning. In Y. Yue, A. Garg, N. Peng, F. Sha, and R. Yu, editors, *International Conference on Representation Learning*, volume 2025, pages 20686–20706, 2025.

[Liu *et al.*, 2020] Yong Liu, Weixun Wang, Yujing Hu, Jianye Hao, Xingguo Chen, and Yang Gao. Multi-agent game abstraction via graph attention neural network. In *AAAI Conference on Artificial Intelligence (AAAI)*, pages 7211–7218, 2020.

[Liu *et al.*, 2023a] Zeyang Liu, Lipeng Wan, Xue Sui, Zhuoran Chen, Kewu Sun, and Xuguang Lan. Deep hierarchical communication graph in multi-agent reinforcement learning. In *International Joint Conference on Artificial Intelligence (IJCAI)*, pages 208–216, 2023.

[Liu *et al.*, 2023b] Zichuan Liu, Yuanyang Zhu, and Chunlin Chen. NA²Q: Neural attention additive model for interpretable multi-agent q-learning. In *International Conference on Machine Learning (ICML)*, pages 22539–22558, 2023.

[Nguyen *et al.*, 2020] Thanh Thi Nguyen, Ngoc Duy Nguyen, and Saeid Nahavandi. Deep reinforcement learning for multiagent systems: A review of challenges, solutions, and applications. *IEEE Transactions on Cybernetics*, 50(9):3826–3839, 2020.

[Ning and Xie, 2024] Zepeng Ning and Lihua Xie. A survey on multi-agent reinforcement learning and its application. *Journal of Automation and Intelligence*, 3(2):73–91, 2024.

[Oroojlooy and Hajinezhad, 2023] Afshin Oroojlooy and Davood Hajinezhad. A review of cooperative multi-agent deep reinforcement learning. *Applied Intelligence*, 53:13677–13722, 2023.

[Orr and Dutta, 2023] James Orr and Ayan Dutta. Multi-agent deep reinforcement learning for multi-robot applications: A survey. *Sensors*, 23(7), 2023.

[Papoudakis *et al.*, 2021] Georgios Papoudakis, Filippos Christianos, Lukas Schäfer, and Stefano V. Albrecht. Benchmarking multi-agent deep reinforcement learning algorithms in cooperative tasks. In *Advances in Neural Information Processing Systems Track on Datasets and Benchmarks (NeurIPS)*, 2021.

[Paszke *et al.*, 2019] Adam Paszke, Sam Gross, Francisco Massa, Adam Lerer, James Bradbury, Gregory Chanan, Trevor Killeen, Zeming Lin, Natalia Gimelshein, Luca Antiga, Alban Desmaison, Andreas Kopf, Edward Yang, Zachary DeVito, Martin Raison, Alykhan Tejani, Sasank Chilamkurthy, Benoit Steiner, Lu Fang, Junjie Bai, and Soumith Chintala. Pytorch: An imperative style, high-performance deep learning library. In *Advances in Neural Information Processing Systems (NIPS)*, volume 32, 2019.

[Rashid *et al.*, 2018] Tabish Rashid, Mikayel Samvelyan, Christian Schroeder de Witt, Gregory Farquhar, Jakob Foerster, and Shimon Whiteson. QMIX: Monotonic value function factorisation for deep multi-agent reinforcement learning. In *International Conference on Machine Learning (ICML)*, pages 1–14, 2018.

[Rashid *et al.*, 2020] Tabish Rashid, Gregory Farquhar, Bei Peng, and Shimon Whiteson. Weighted QMIX: Expanding monotonic value function factorisation for deep multi-agent reinforcement learning. In *Advances in Neural Information Processing Systems (NeurIPS)*, pages 1–20, 2020.

[Samvelyan *et al.*, 2019] Mikayel Samvelyan, Tabish Rashid, Christian Schroeder de Witt, Gregory Farquhar, Nantas Nardelli, Tim G. J. Rudner, Chia-Man Hung, Philip H. S. Torr, Jakob Foerster, and Shimon Whiteson. The StarCraft Multi-Agent Challenge. *CoRR*, abs/1902.04043, 2019.

[Schmidt *et al.*, 2022] Lukas M. Schmidt, Johanna Brosig, Axel Plinge, Bjoern M. Eskofier, and Christopher Mutschler. An introduction to multi-agent reinforcement learning and review of its application to autonomous mobility. In *International Conference on Intelligent Transportation Systems (ITSC)*, pages 1342–1349, 2022.

[Son *et al.*, 2019] Kyunghwan Son, Daewoo Kim, Wan Ju Kang, David Earl Hostallero, and Yung Yi. QTRAN: Learning to factorize with transformation for cooperative multi-agent reinforcement learning. In *International Conference on Machine Learning (ICML)*, pages 1–18, 2019.

[Sukhbaatar *et al.*, 2016] Sainbayar Sukhbaatar, Arthur Szlam, and Rob Fergus. Learning multiagent communication with backpropagation. In *Advances in Neural Information Processing Systems (NIPS)*, volume 29, 2016.

[Sunehag *et al.*, 2018] Peter Sunehag, Guy Lever, Audrunas Gruslys, Wojciech Marian Czarnecki, Vinicius Zambaldi, Max Jaderberg, Marc Lanctot, Nicolas Sonnerat, Joel Z. Leibo, Karl Tuyls, and Thore Graepel. Value-decomposition networks for cooperative multi-agent learning based on team reward. In *International Conference on Autonomous Agents and Multiagent Systems (AAMAS)*, pages 2085–2087, 2018.

[Sutton and Barto, 2018] Richard S. Sutton and Andrew G. Barto. *Reinforcement Learning: An Introduction*. The MIT Press, second edition, 2018.

[Tan *et al.*, 2024] Weihao Tan, Wentao Zhang, Shanqi Liu, Longtao Zheng, Xinrun Wang, and Bo An. True knowledge comes from practice: Aligning large language models with embodied environments via reinforcement learning. In *International Conference on Learning Representations (ICLR)*, 2024.

[Tieleman and Hinton, 2012] S. Tieleman and G. Hinton. Lecture 6.5—RMSProp: Neural networks for machine learning. *COURSERA Technical Report*, 2012.

[Vaswani *et al.*, 2017] Ashish Vaswani, Noam Shazeer, Niki Parmar, Jakob Uszkoreit, Llion Jones, Aidan N. Gomez, Łukasz Kaiser, and Illia Polosukhin. Attention is all you need, 2017. arXiv:1706.03762.

[Wang *et al.*, 2019] Tonghan Wang, Jianhao Wang, Chongyi Zheng, and Chongjie Zhang. Learning nearly decomposable value functions via communication minimization. In *International Conference on Learning Representations (ICLR)*, 2019.

[Wang *et al.*, 2021] Jianhao Wang, Zhizhou Ren, Terry Liu, Yang Yu, and Chongjie Zhang. QPLEX: Duplex dueling multi-agent q-learning. In *International Conference on Learning Representations (ICLR)*, pages 1–27, 2021.

[Wang *et al.*, 2022] Jianhong Wang, Yuan Zhang, Yunjie Gu, and Tae-Kyun Kim. Shaq: Incorporating shapley value theory into multi-agent q-learning. In *Advances in Neural Information Processing Systems (NeurIPS)*, volume 35, pages 5941–5954, 2022.

[Wong *et al.*, 2023] Annie Wong, Thomas Bäck, Anna V. Kononova, and Aske Plaat. Deep multiagent reinforcement learning: challenges and directions. *Artificial Intelligence Review*, 56:5023–5056, 2023.

[Yadav *et al.*, 2023] Pamul Yadav, Ashutosh Mishra, and Shiho Kim. A comprehensive survey on multi-agent reinforcement learning for connected and automated vehicles. *Sensors*, 23(10), 2023.

[Yang *et al.*, 2020] Yaodong Yang, Jianye Hao, Ben Liao, Kun Shao, Guangyong Chen, Wulong Liu, and Hongyao Tang. Qatten: A general framework for cooperative multi-agent reinforcement learning, 2020. arXiv:2002.03939.

[Yuan *et al.*, 2022] Lei Yuan, Jianhao Wang, Fuxiang Zhang, Chenghe Wang, Zongzhang Zhang, Yang Yu, and Chongjie Zhang. Multi-agent incentive communication via decentralized teammate modeling. In *AAAI Conference on Artificial Intelligence (AAAI)*, pages 9466–9474, 2022.

A Detailed Results

A.1 Main results

Figures 5, 6, 7, 8, and 9 contain training curves of our experiments described in Section 4.4. The curves on the plots represent the mean percentage test game win rate during the algorithm training for different environments and various mixers. The shaded area around the curves is the standard deviation of the results among 5 different seeds (1 to 5) of the random number generator. For each seed, the mean percentage test win rate was calculated based on 32 independent test episodes.

SMACv2. MACTAS performs the best on most maps. MASIA performs really good on a few maps (like `protoss_20_vs_23` with the QMIX mixer), but does not outperform the bare mixer on a number of maps (like `terran_5_vs_5` and `protoss_5_vs_5` with all mixers, `terran_10_vs_11` with QPLEX and VDN). MAIC performs on par with MACTAS or MASIA on a few maps, but does not visibly outperform other methods on any map. Moreover, MAIC+QPLEX in some runs fails to complete the training – the runs output “NaN” in the network weights (we use the official implementation provided by the MAIC authors). For such cases, we report the last value before the algorithm’s failure as its output from that timestep to the end of the training.

SMAC. MACTAS with the QMIX mixer outperforms baselines on the most challenging environments `6h_vs_8z` and `3s5z_vs_3s6z` by a large margin. MASIA excels on the `27m_vs_30m` and `MMM2` map, but fails to solve not only the two most challenging maps, but also a simple `2c_vs_64zg`. MAIC does not degenerate in a similar way to MASIA, but visibly outperforms MACTAS only on the `MMM2` map.

LBF and Hallway. On the LBF and Hallway benchmarks with the QMIX mixer, MASIA learns the fastest, but MACTAS solves both tasks as well. MAIC and the bare mixer solve the LBF task, but fail to solve the Hallway benchmark.

A.2 MAIC+QPLEX errors

We observe that MAIC+QPLEX results in NaN errors in some runs. As mentioned before, in such cases, we report the last value before the algorithm’s failure as its output from that timestep to the end of the training. In Table 3, we report which seeds returned this error, after how many training steps the algorithm returned it, and the last value outputted by the algorithm.

A.3 Robustness study

As RL algorithms are studied in synthetic environments, many of the challenges encountered when applying these algorithms in the real world are not properly represented. In terms of MARL, algorithms are usually designed to maximize the speed of learning in a range of predefined environments, executing both the environment and the algorithm code together on a single machine. This setup can be hard to replicate in many real-world scenarios, where each agent is physically autonomous and performs all computation on embedded hardware, while communication with its peers needs to

Map name	Seed	Last score	Last step (million)	Total environment steps (million)
terran_10_vs_11	4	0.0%	6.58	7.50
terran_20_vs_23	2	0.0%	5.66	7.50
terran_20_vs_23	3	0.0%	2.55	7.50
zerg_10_vs_11	3	0.0%	6.29	7.50
zerg_20_vs_23	1	0.0%	4.45	7.50

Table 3: The seeds that returned the NaN error for MAIC+QPLEX on the SMACv2 benchmark.

be performed over radio communication with volatility and disruptions.

We consider robustness an important aspect of algorithm design, thus testing MACTAS against such adversary conditions. The exact artifacts that may arise from communication channel instability vary depending on the media and protocol, but assuming proper error detection, they all result in the agents’ inability to exchange messages for prolonged periods of time. To simulate this, we perturb the Transformer source mask, resulting in blocking agent pairs from exchanging information in a sequence of time steps. The exact algorithm is described in the main part of the paper.

We specifically do not introduce any modifications to MACTAS learning algorithm, making it unaware of the disruptions. The attention masking matrix is not memorized as part of the state, and is not given to the model as an input during inference or during training. Figure 10 presents the results of various disruption probabilities p across four SMACv1 environments. In one of them, with only 2 agents, `2v_vs_64zg`, the disruption doesn’t impact the scores, indicating that communication is not required to solve the environment. In three other, MACTAS performs consistently, demonstrating strong performance for up to 60% of disruption.

The results indicate that without any changes to the algorithm, MACTAS could be deployed in conditions of up to 60% variable time, pair-wise connection loss, and show strong learning performance.

A.4 Ablations

Residual connection. We study the importance of the extra residual connection in the architecture of MACTAS. We show the comparison of performance with and without this residual connection with QMIX as the mixer on SMAC in Figure 11. We observe that, on the most challenging maps (`6h_vs_8z` and `3s5z_vs_3s6z`), the architecture with the residual connection becomes important, whereas the architecture without the residual connection remains robust on four simpler tasks.

Domain randomization. We observe that MACTAS advantage over other algorithms is most visible in difficult SMACv2 benchmarks. What distinguishes it from SMAC is that the positions and types of both teammates and enemies

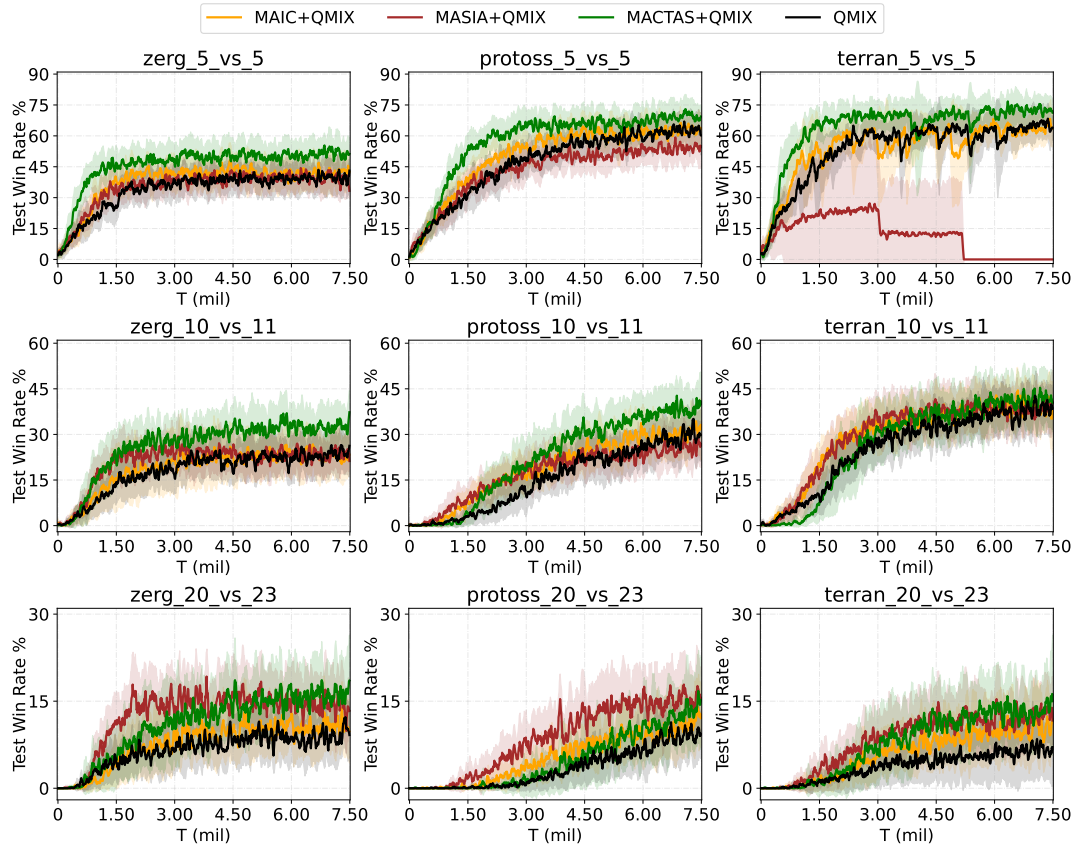


Figure 5: Means and standard deviations of the percentage wins in the test games during training for QMIX with MACTAS, MAIC, MASIA, and the bare mixer for the SMACv2 benchmark.

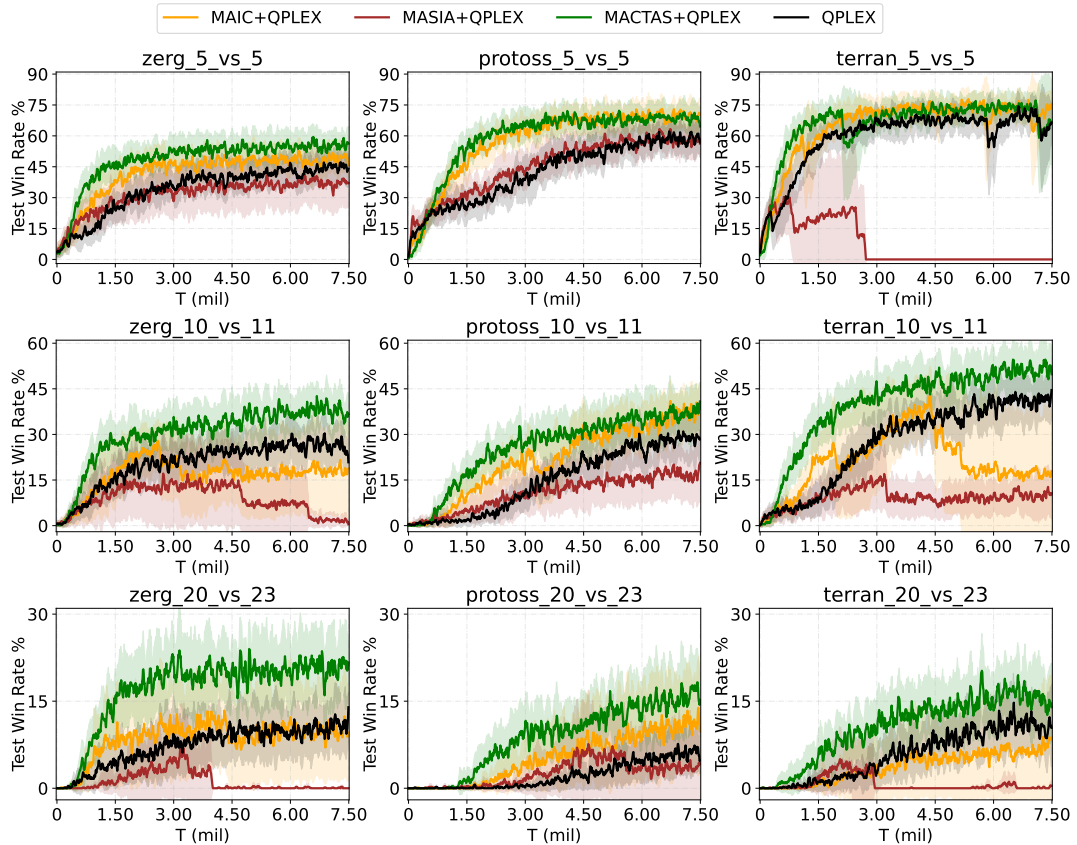


Figure 6: Means and standard deviations of the percentage wins in the test games during training for QPLEX with MACTAS, MAIC, MASIA, and the bare mixer for the SMACv2 benchmark.

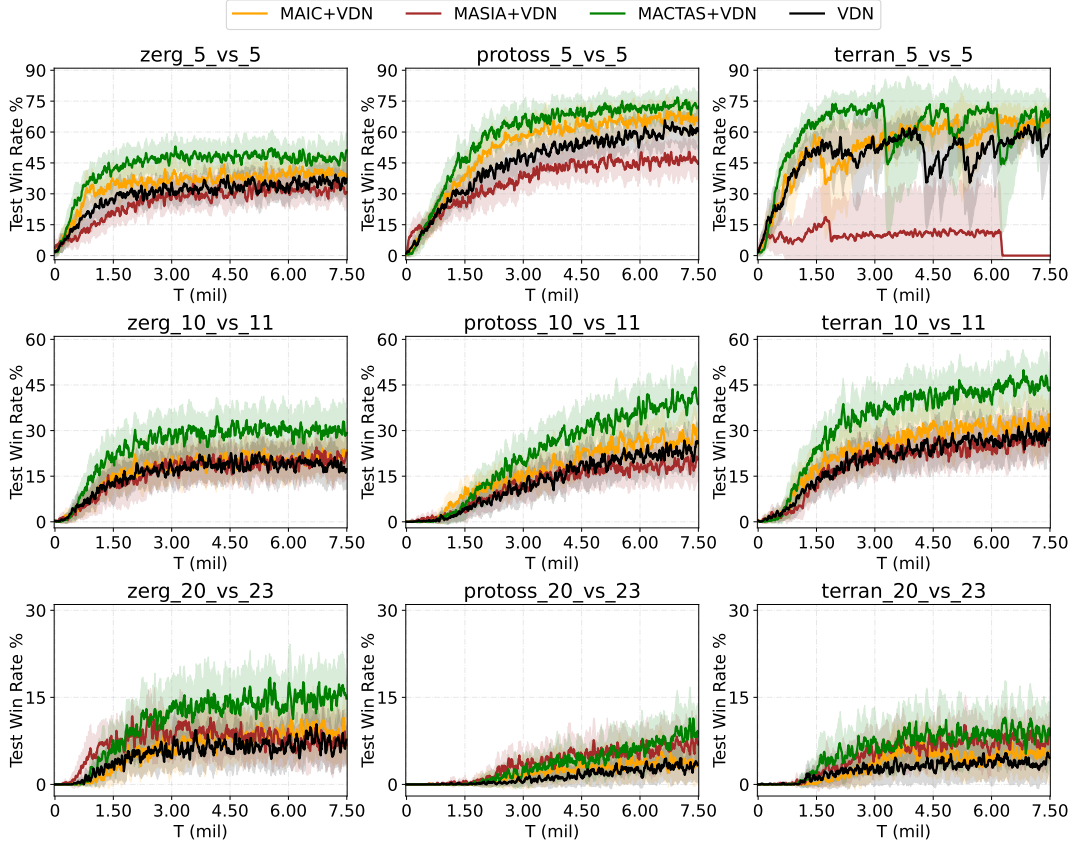


Figure 7: Means and standard deviations of the percentage wins in the test games during training for VDN with MACTAS, MAIC, MASIA, and the bare mixer for the SMACv2 benchmark.

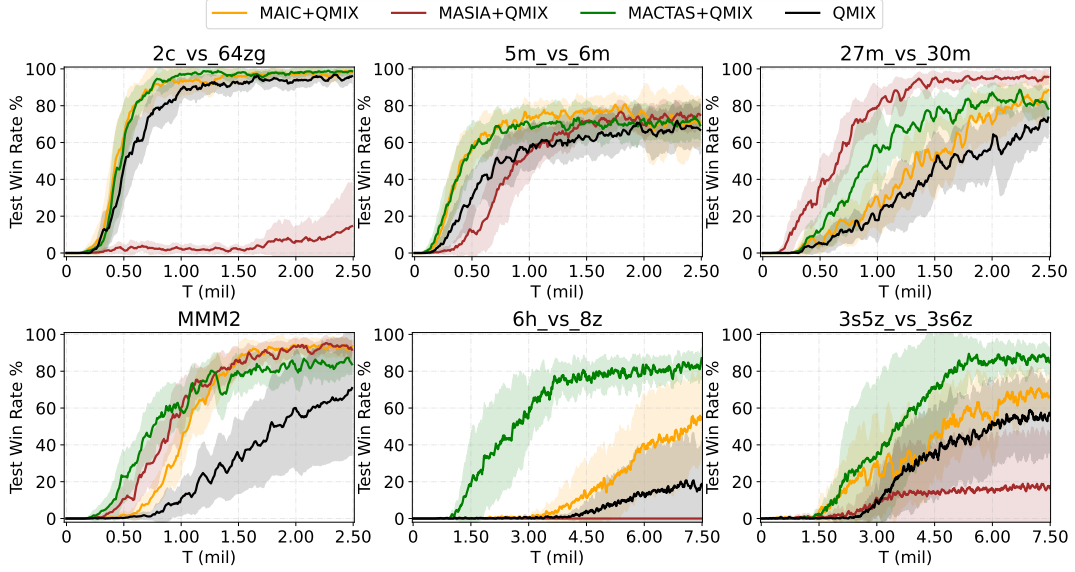


Figure 8: Means and standard deviations of the percentage wins in the test games during training for QMIX with MACTAS, MAIC, MASIA, and the bare mixer for the SMAC benchmark.

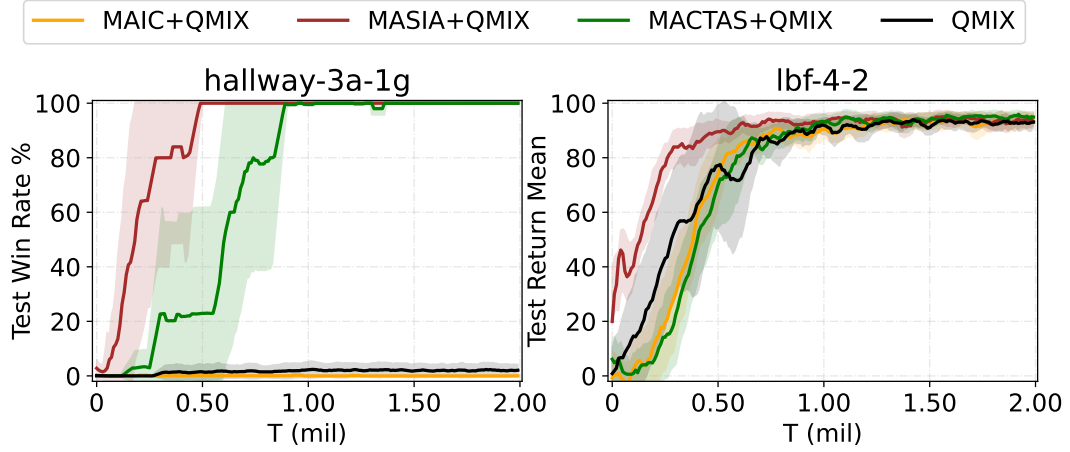


Figure 9: Means and standard deviations of the percentage wins in the test games during training for QMIX with MACTAS, MAIC, MASIA, and the bare mixer for the Hallway and LBF benchmarks.

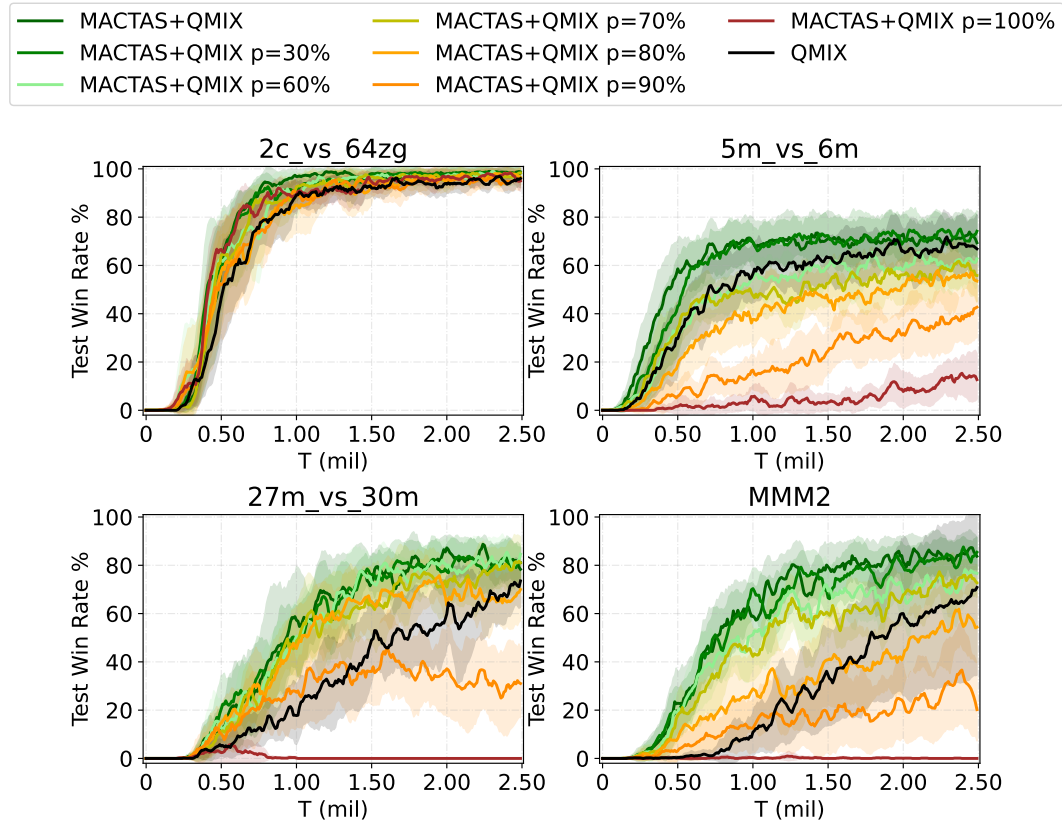


Figure 10: Means and standard deviations of the percentage wins for the connectivity disruption simulation at different p values in the test games during training for QMIX with MACTAS for the SMAC benchmark.

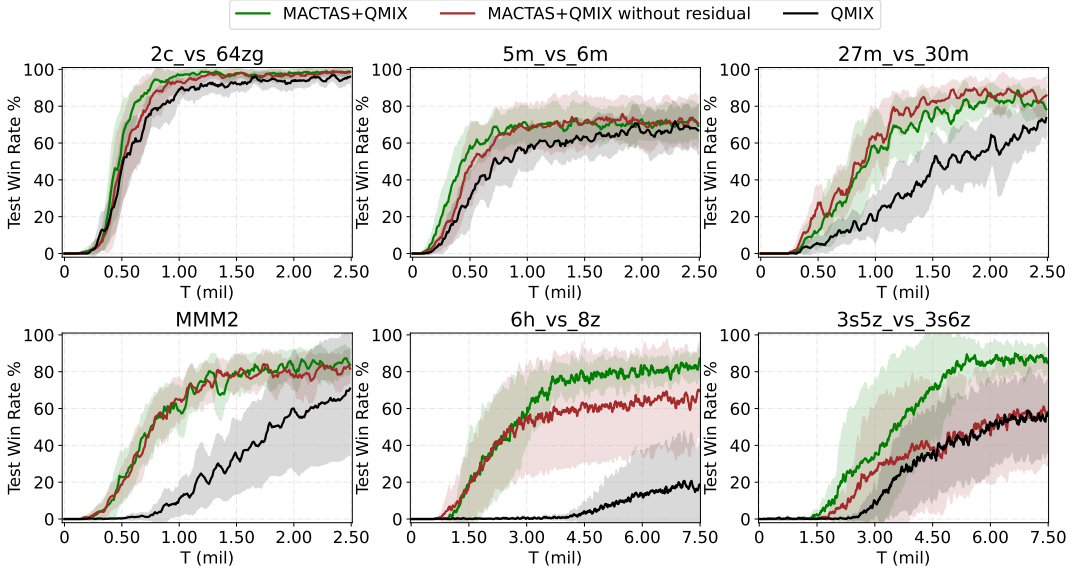


Figure 11: Means and standard deviations of the percentage wins in the test games during training for QMIX with MACTAS with and without the extra residual connection for the SMAC benchmark.

are re-randomized in every episode. This makes both teammate modeling (MAIC) and joint-state modeling (MASIA) harder due to a vastly larger state domain and increased variance of the inputs. To verify this, we set up an experiment in which we modify the SMACv2 environment behaviour so that units' positions/types remain randomized for each global seed, but remain static for all episodes of that seed. This essentially removes the stochasticity of the SMACv2 environment, making the agent's configuration static throughout the learning process. We observe that in this setup, MASIA can level the performance of MACTAS on the SMACv2 maps with 5 agents, on which MACTAS outperforms MASIA by a large margin when randomization is present. The training curves are presented in Figure 12. We conclude that the advantages of MACTAS are particularly evident in complex tasks, where the agent must adapt to different scenarios rather than learn a policy for a fixed scenario.

A.5 QPLEX variants

We note that the QPLEX mixer [Wang *et al.*, 2021] is presented in two variants: with the MLP and the attention architecture. For MACTAS, we chose the MLP variant and compared it with the MLP variant of QPLEX. However, MASIA and MAIC use the attention variant, and we followed their choice in the main experiments. We study how MACTAS+QPLEX and QPLEX perform if we change the architecture to the attention one. The results are presented in Figure 13. We observe that for MACTAS the attention variant performs similarly on the most maps, better on the protoss_20_vs_23 and worse on the zerg_20_vs_23 and terran_20_vs_23 maps. The attention variant for the QPLEX usually performs not worse than the MLP variant, but fails on the terran_20_vs_23 map. We observe that MACTAS+QPLEX with the attention architecture outperforms QPLEX with the attention architec-

ture, MASIA, and MAIC.

B Sensitivity analysis

We observe that MACTAS is moderately sensitive to the architecture choice of the Transformer encoder, namely, the number of stacked layers of the Transformer encoder and the dimension of the feedforward network (we use in all experiments $d_{model} = 64$, as it should be equal to the RNN hidden dimension). We use a consistent architectural choice for the most challenging benchmarks (all SMACv2 maps and two SMAC maps: 3s5z_vs_3s6z, 6h_vs_8z), and the toy problems (LBF and Hallway). For the remaining four SMAC maps, we use the same architecture for 27m_vs_30m, 5m_vs_6m, and a separate one 2c_vs_64zg and MMM2. We present a study of the robustness of MACTAS across different architectural choices with QMIX as the mixer. We denote by "lx dimffy" the architecture with x layers and the size of the feedforward network hidden layer equal to y .

B.1 SMACv2

We show the sensitivity of MACTAS to the number of Transformer encoder layers with the size of the feedforward hidden layer equal to 512 in Figure 14. On the SMACv2 benchmark, we observe that MACTAS performs well with the default architecture. On some maps (terran_10_vs_11, protoss_20_vs_23), one can slightly improve the results by taking a different number of layers. All tested number of layers perform not worse than the bare mixer, apart from the case of one layer on the zerg_20_vs_23 map.

B.2 SMAC

As MACTAS is more sensitive to the architectural choice on SMAC, we show the whole hyperparameter search. We

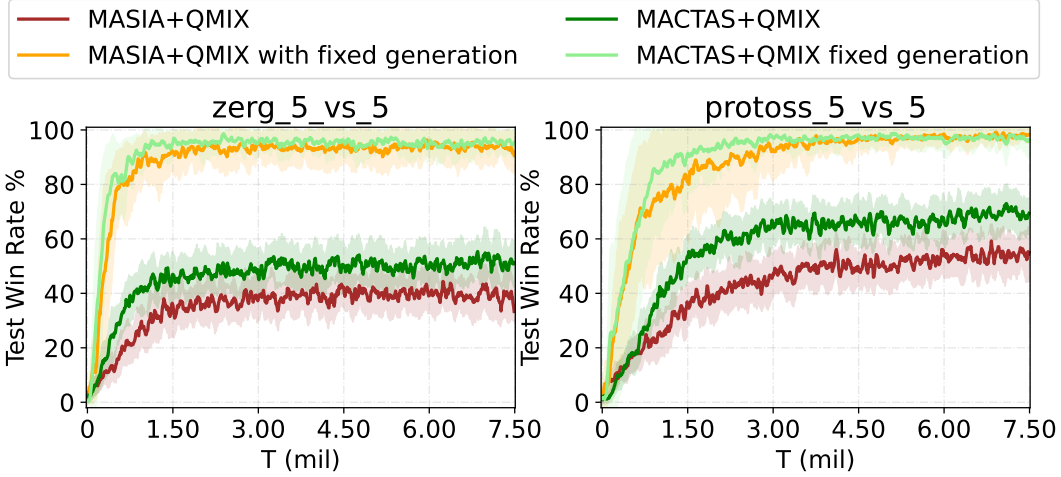


Figure 12: Means and standard deviations of the percentage wins in the test games during training for QMIX with MACTAS and MASIA with full randomization and fixed episode generation for two SMACv2 maps.

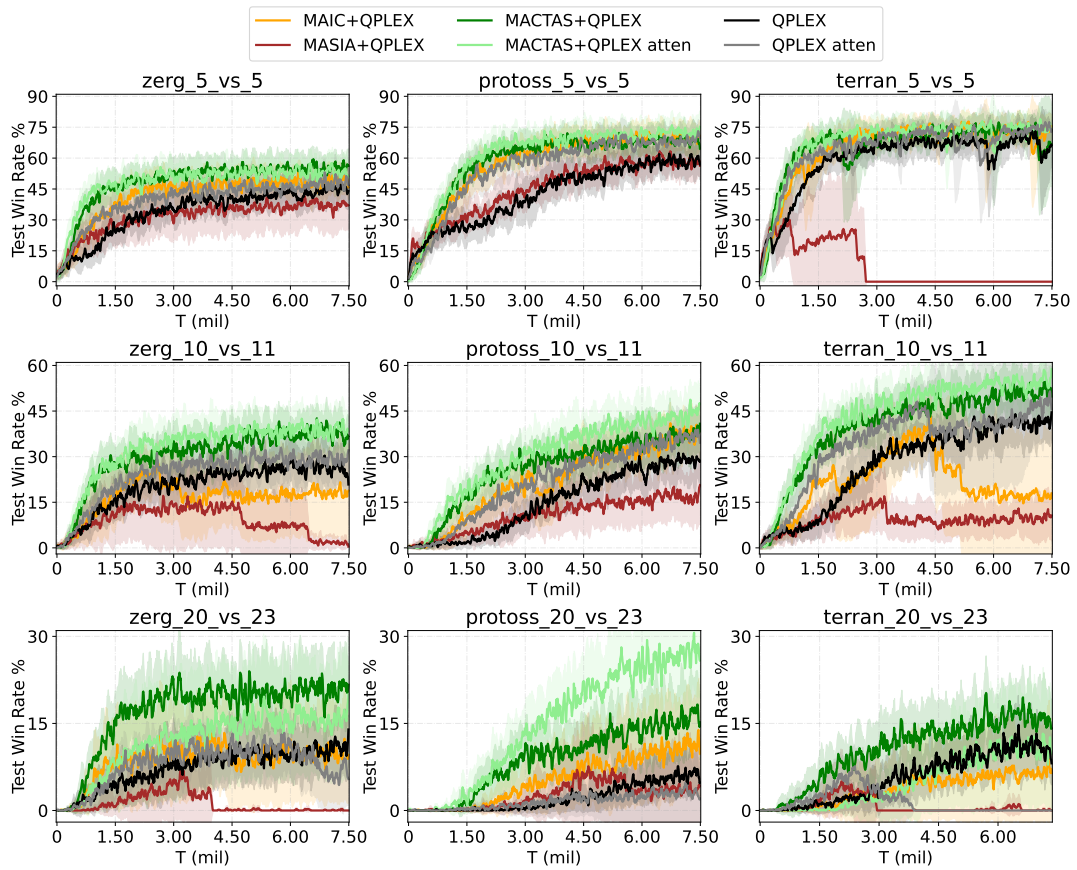


Figure 13: Means and standard deviations of the percentage wins in the test games during training for MACTAS+QPLEX and QPLEX with the MLP and the attention QPLEX architecture for the SMACv2 maps.

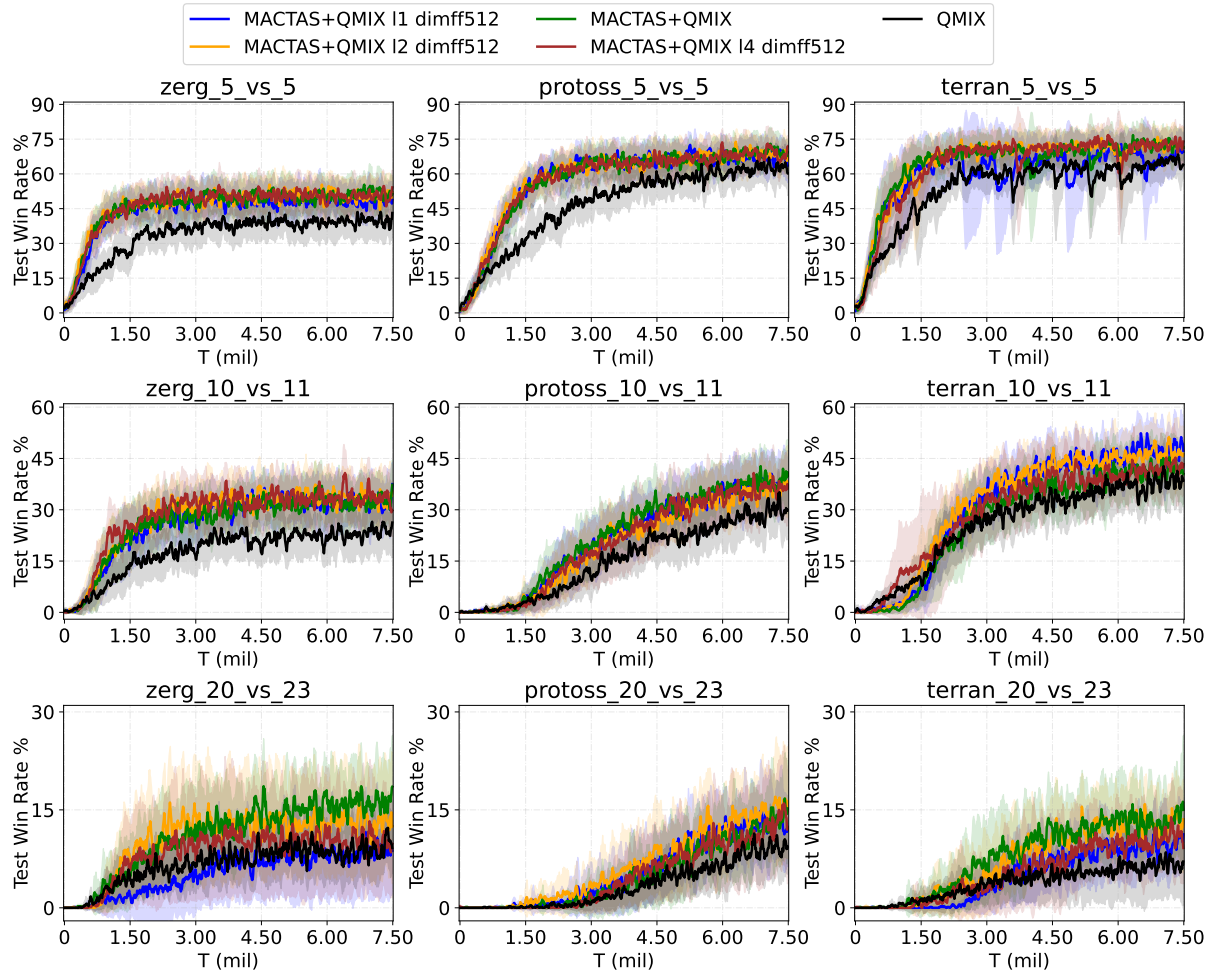


Figure 14: MACTAS; sensitivity of the results to architecture size with the QMIX mixer on the SMACv2 benchmark.

test the one, two, three, and four stacked Transformer encoder layers and the dimension of the Transformer feedforward network equal to 128, 256, 512, and 1024. The results are presented in Figures 15, 16, 17, and 18. We observe that MACTAS performs not worse than the bare mixer in almost all tested configurations and scenarios. On the `2c_vs_64zg` and `5m_vs_6m` maps, most of the setups perform equally well. On the remaining maps, the architectural choice is important, but there are alternative settings performing similarly to the optimal architecture (for example, `11dimff1024`, `13dimff1024`, `14dimff1024` on the `6h_vs_8z` map; `12dimff512` on the `3s5z_vs_3s6z` map).

B.3 LBF and Hallway

On the simple tasks, MACTAS requires a small Transformer architecture to learn fast. Thus, for the toy problems, we choose the one-layer architecture. We test the Transformer encoder with feedforward network widths of 32, 64, and 128. The results are presented in Figure 9. We observe that one can obtain even better results on the Hallway by selecting a slightly different architecture, but we aim to keep the architecture consistent across the toy problems.

C StarCraft Multi-Agent Challenge (SMAC & SMACv2)

As a benchmark for MACTAS, we chose the StarCraft Multi-Agent Challenge (SMAC) [Samvelyan *et al.*, 2019] and its newer version SMACv2 [Ellis *et al.*, 2023], which are simplified versions of the StarCraft II game. The framework exists in two versions – SMAC (code available at <https://github.com/oxwhirl/smac>), which introduced predefined deterministic scenarios that often include purposeful selection of units or obstacles placement, and SMACv2 (code available at <https://github.com/oxwhirl/smav2>), which added new randomized scenarios based on plain maps and randomized units generation. From here onward, we will use "SMACv1" to refer to the first version of the benchmark and "SMAC" to refer to both SMACv1 and SMACv2, making an explicit distinction where necessary. SMAC uses PySc2 to communicate with the game engine <https://github.com/google-deepmind/pysc2>. SMAC is characterized by the decentralized management of each unit, where each unit acts as an independent agent. This feature allows for the testing of decentralized algorithms, including those originating from MARL. Benchmark scenarios are limited to combat with a limited number of units. Those scenarios do not account for the economic aspect of the game, the so-called "macro" part of the game – collecting resources and building structures. Resources in the game (gas and minerals) are required to build units and structures. Structures enable the recruitment of units and their subsequent upgrading. The considered scenarios do not involve "worker" units, which collect resources. Instead, the scenarios focus on 'micro', a term used in the StarCraft II community to describe unit control during combat. In SMACv2, the new addition is randomized maps defined by race (same for both teams), number of units in each team, thus map names like `zerg_10_vs_11`. The new maps randomize types of units according to the probability of each unit type defined in

Hyperparameter	Value
Batch size	32
Test episodes	32
Replay buffer size	5000
Discount factor	0.99
Start epsilon	1.0
Finish epsilon	0.05
Anneal steps	50,000 ¹ or 100,000 ²
RNN units	64
Optimizer	RMSProp
Learning rate	0.0005

Table 4: Basic experimental settings and hyperparameters. ¹ for LBF, Hallway, and 2.5-million step SMAC maps. ² for SMACv2 and 7.5 million-step SMAC maps.

Library name	Version
Python	3.9.21 or 3.9.22
numpy	1.23.1
nvidia-cublas-cu12	12.4.5.8
nvidia-cuda-cupti-cu12	12.4.127
nvidia-cuda-nvrtc-cu12	12.4.127
nvidia-cuda-runtime-cu12	12.4.127
nvidia-cudnn-cu12	9.1.0.70
nvidia-cufft-cu12	11.2.1.3
nvidia-curand-cu12	10.3.5.147
nvidia-cusolver-cu12	11.6.1.9
nvidia-cusparse-cu12	12.3.1.170
nvidia-ncc1-cu12	2.21.5
nvidia-nvjitlink-cu12	12.4.127
nvidia-nvtx-cu12	12.4.127
scipy	1.13.1
torch	2.5.1

Table 5: Essential libraries in programming environment.

scenario configuration files called capabilities config. In addition, the configuration allows for specifying the units' start position, their spread, and configuration – either surround, reflect, or random probability of each. The challenge for a human player is to multitask between these two tasks – developing the game economy and controlling the fighting units. SMAC focuses solely on combat, thereby ensuring repeatability of this benchmark, as each iteration involves a fight between the same specification units, eliminating uncertainty due to unit upgrades and different strategies in the economic part of the game. In StarCraft II, there are three races, and our experiments covered controlling units of all of them. The process for running SMAC is described in our repository.

D Setup hyperparameters

All hyperparameters not strictly related to the communication algorithm are shared between maps, algorithms, and mixers and are presented in Table 4.

E Tactics used by MACTAS

The SMAC challenge forces agents to learn various tactics, such as attacking from a distance with melee units ('kiting')

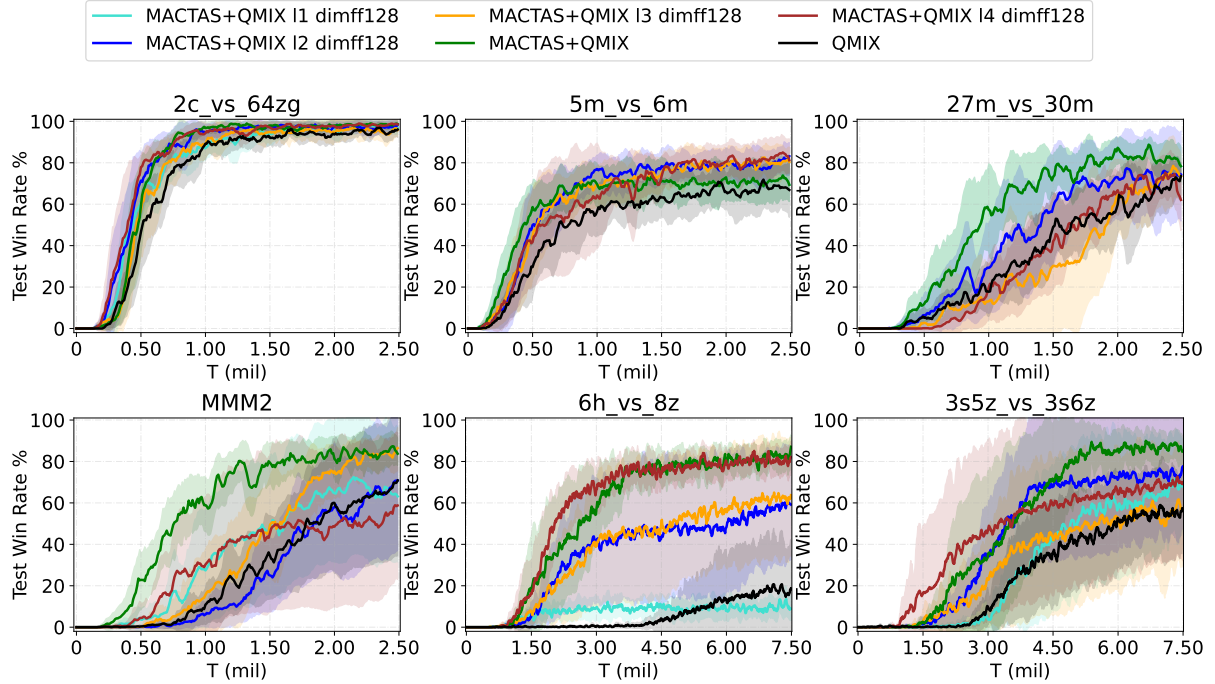


Figure 15: MACTAS; sensitivity of the results to architecture size with the QMIX mixer and the size of the feedforward connection equal to 128 and optimal on the SMAC benchmark.

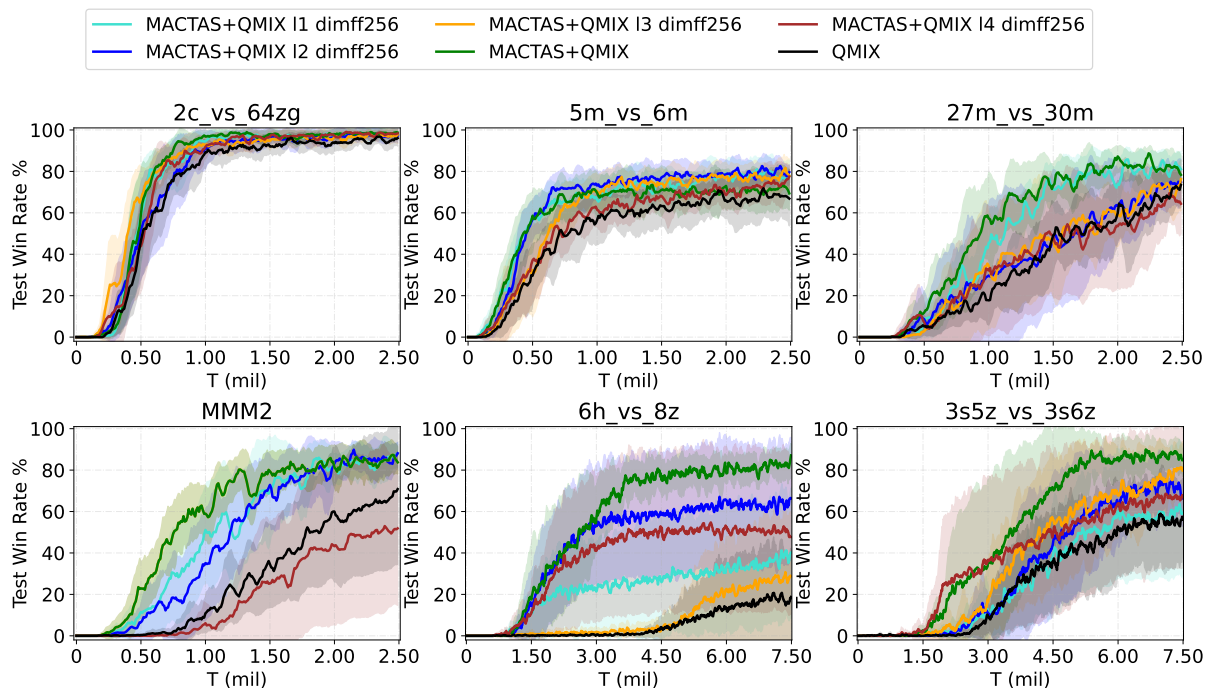


Figure 16: MACTAS; sensitivity of the results to architecture size with the QMIX mixer and the size of the feedforward connection equal to 256 and the optimal architecture on the SMAC benchmark .

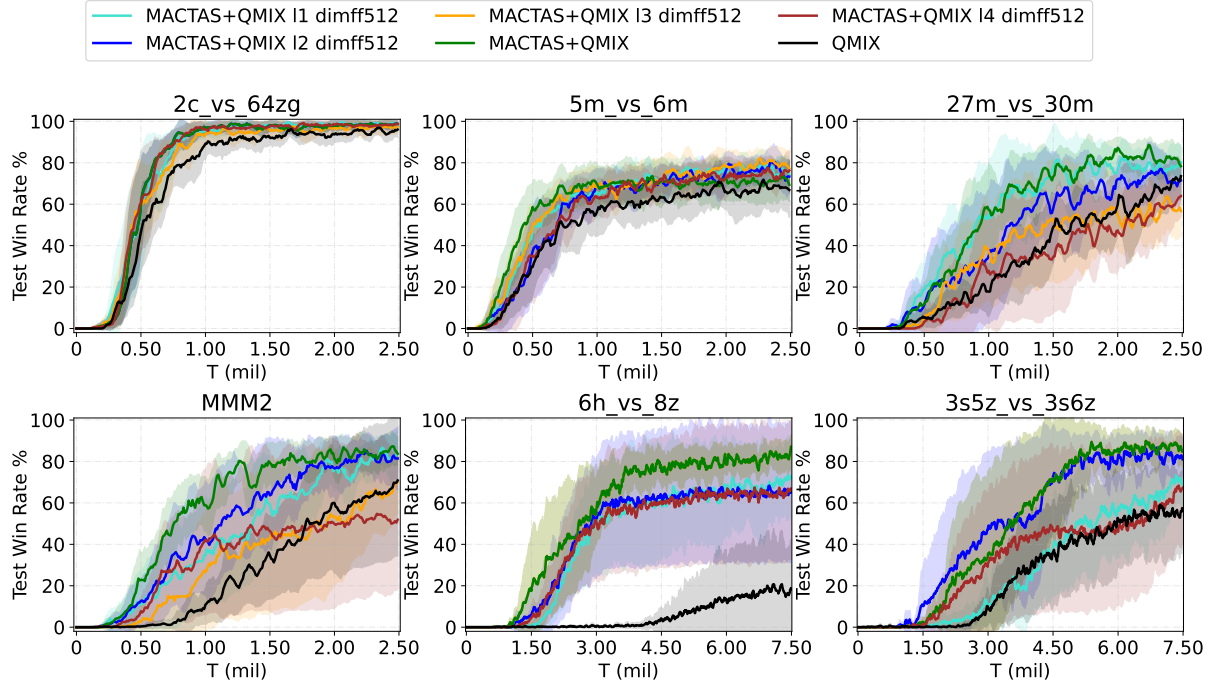


Figure 17: MACTAS; sensitivity of the results to architecture size with the QMIX mixer and the size of the feedforward connection equal to 512 and the optimal architecture on the SMAC benchmark .

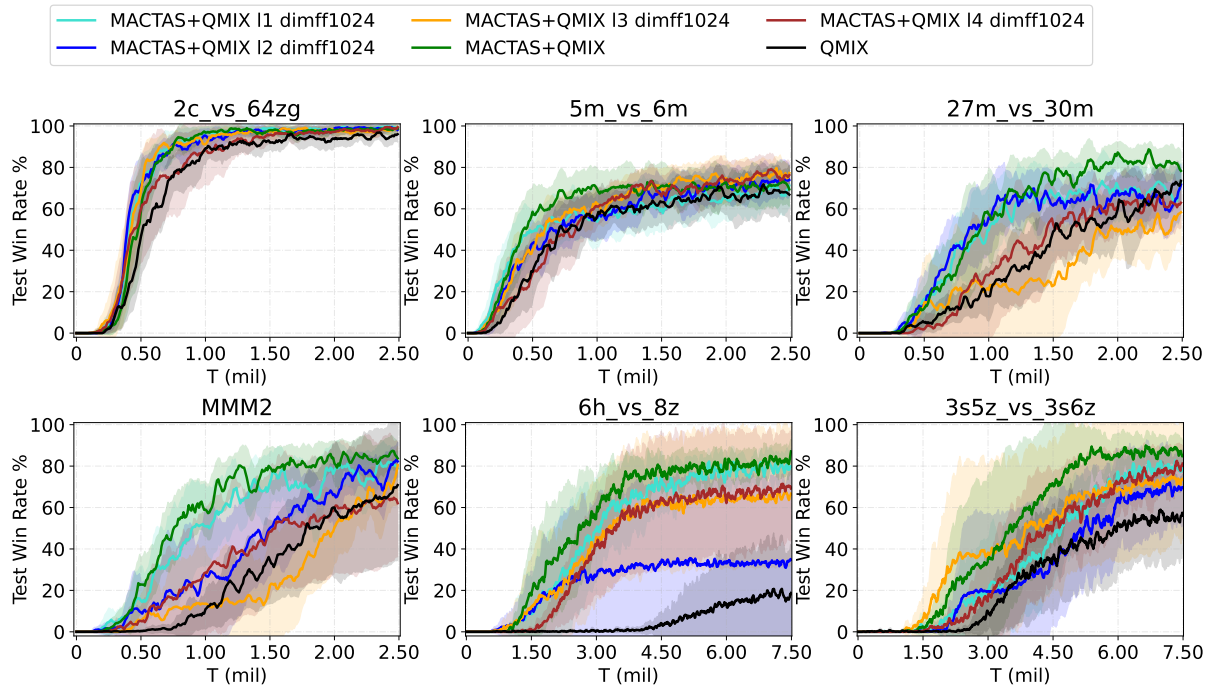


Figure 18: MACTAS; sensitivity of the results to architecture size with the QMIX mixer and the size of the feedforward connection equal to 1024 and the optimal architecture on the SMAC benchmark.

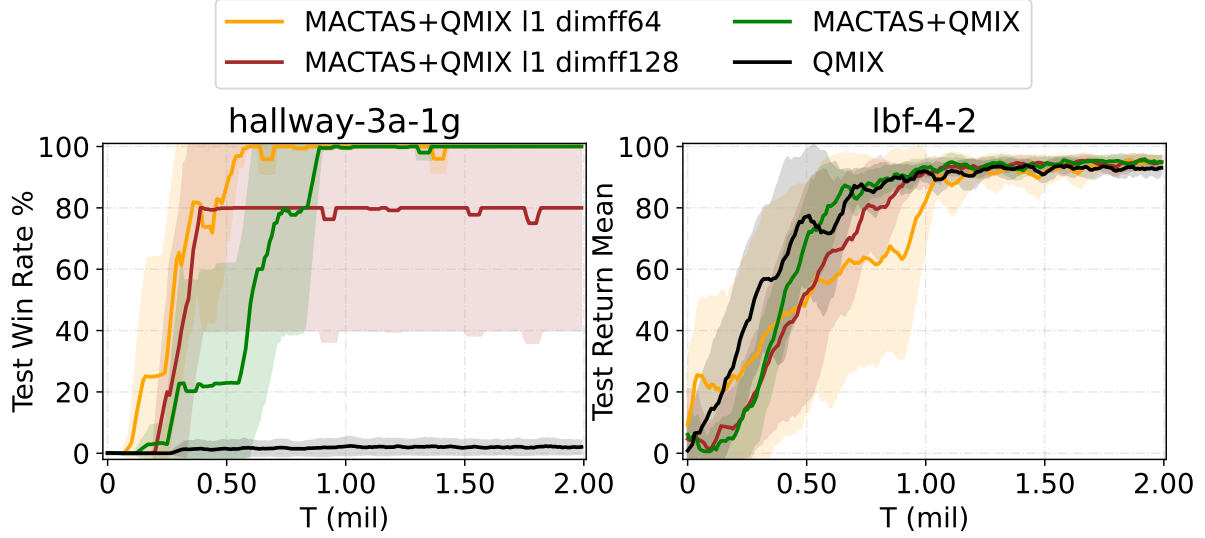


Figure 19: MACTAS; sensitivity of the results to architecture size with the QMIX mixer and one-layer architecture on the Hallway and LBF benchmarks.

Cluster name	GPU device	GPU driver version	CPU device	Operating system	Total RAM
Cluster 1	NVIDIA A100 SXM4 80GB	535.154.05	AMD EPYC 7742 64-Core Processor	Linux-5.15.0-1059-nvidia-x86_64-with-glibc2.35	1024 GB
Cluster 2	NVIDIA A100 SXM4 40GB	570.133.20	AMD EPYC 7742 64-Core Processor	Linux-5.14.0-503.26.1.el9_5.x86_64-x86_64-with-glibc2.34	1024 GB
Cluster 3	NVIDIA A100 PCIe 80GB	565.57.01	AMD EPYC 7713 64-Core Processor	Linux-6.8.0-64-generic-x86_64-with-glibc2.39	2048 GB

Table 6: Specification of the computational clusters used in the experiments.

or using a movement advantage ('hit and run'). In this section, we provide an overview of the tactics used by our model based on our understanding of StarCraft II. We observed differences in the behavior of our model depending on the random seed. The description of tactics is based on replays of our models for a seed value of 1.

We describe tactics on the following maps from SMACv1:

- 2c_vs_64zg with 2 colossus units leveraging terrain advantage against 64 small enemy zerglings. Level: hard.
- 5m_vs_6m with 5 cooperating marines and 6 enemy marines. Level: hard.
- 27m_vs_30m big battle of 27 marines conquering 30 marines. Level: super-hard.
- MMM2 scenario with diverse units containing 1 medivac (medic), 2 marauders, and 7 marines fighting team with 1 more marauder and 1 more marine. Level: super-hard.
- 6h_vs_8z with 6 shooting hydralisks against 8 malee zealots. Level: super-hard.



Figure 20: 2c_vs_64zg replay.

- 3s5z_vs_3s6z scenario with 3 stalkers and 5 zealots against 3 stalkers and 6 zealots. Level: super-hard.



Figure 21: 27m_vs_30m replay.



Figure 22: 5m_vs_6m replay.

E.1 2c_vs_64zg

In this scenario, agents control 2 colossi units. Colossi can move through hills between the high and the low ground. Against them, 64 enemy zerglings are deployed, which are fast ground units. Zerglings are most effective when they surround an opposite unit. In the scenario 2c_vs_64zg, the colossi start on the hill, while the zerglings are split into two groups of 32 on the left and the right, both of them on the low ground. Figure 20 presents the following tactics: colossi attack the right group of zerglings and wait for the left group to climb the hill. Then, colossi use the ability to traverse the hill and attack the remaining zerglings, which are forced to run around the hill. In this way, the colossi avoid being surrounded and thereby defeated.

E.2 27m_vs_30m and 5m_vs_6m

The 27m_vs_30m and the 5m_vs_6m scenarios consist of marine units only. They are similar in the way that the opposing force numerically outnumbers the agents under control. In Figure 21, the agent's units place themselves in a semi-circle formation, also known as flanking, which maximizes the number of shooting units, while the enemies block each other. Units controlled by MACTAS focus fire on enemy units with lower health to quickly reduce the number of opponents. Furthermore, units with low health retreat and continue fighting, while avoiding being shot. This behavior is presented in Figure 22: Agents with low health retreat when others focus fire on one enemy unit. The winning strategy is similar for both



Figure 23: MMM2 replay.

5m_vs_6m and 27m_vs_30m. 5m_vs_6m is labeled as a hard benchmark, while 27m_vs_30m is classified as super-hard. The percentage imbalance between units is higher in 5m_vs_6m. However, 27m_vs_30m has a larger number of units that need to cooperate.

E.3 MMM2

The MMM2 is a scenario with a diverse set of units containing 1 medivac (medic), 2 marauders, and 7 marines fighting against a team with 1 more marauder and 1 more marine. Medivac cannot attack, but can heal units as long as it has energy. MACTAS ground units focus fire on enemy units and eliminate them one by one, and fall back when their health is low. The enemy medivac does not change healed unit, while the MACTAS' medivac changes healed unit to the one with a critically low health or to the currently attacked unit. Units trained with MACTAS move medivac to the front line and focus enemy fire on it, and when its health level is low, retreat it. MACTAS' medivac taking enemy fire secures outnumbered marines and marauders. Typically, human players try to save their medivacs because they are used for healing units between fights during a regular game. Only under certain conditions do they sacrifice their medivacs; for example, when they are breaking through an opponent's line of defense to focus enemy fire on the medivacs and away from damage-dealing units. In this scenario, we can observe similar behavior in the MACTAS medivac control, which results in winning combat against an opponent who has a numerical advantage.

E.4 6h_vs_8z

Agents control 6 range shooting units, hydralisks, while the enemy controls 8 melee zealots. In Figure 24, we can see a tactic called “kiting” – hydralisks split into two groups and are attacking zealots from distances. Enemy zealots attack the nearest unit – our agents learned to move enough to change the focus of approaching units and then continue striking. Notably, the zealot units within this scenario are not upgraded with the “charge” ability, which would otherwise allow them to have a significant increase in movement speed and easily reach hydralisks.

E.5 3s5z_vs_3s6z

MACTAS controls 3 stalkers and 5 zealots, while the enemy has one more zealot. The stalkers are fast, range-attacking



Figure 24: 6h_vs_8z replay.



Figure 25: 3s5z_vs_3s6z replay.

units, but with weak defense. On the other hand, zealots have a good defense, but they need to get close to the opponent’s unit. The tactic in this scenario is interesting. Using one stalker as a decoy, MACTAS first defeats the enemy stalkers and then proceeds to eliminate the rest of the enemy force. One agent, a stalker, sacrifices himself and focuses a few enemy zealots on himself. In Figure 25, we can see 5 enemy zealots following the stalker marked as “Local Player”. The remaining MACTAS’ 2 stalkers and 5 zealots attack 3 enemy stalkers and 1 zealot with an advantage. This move results in the elimination of enemy stalkers and the zealot. In the end, MACTAS’ units eliminate zealots lured by the sacrificed stalker.

F Software

Table 5 contains a list of key programming libraries used during our experiments. The complete list of programming libraries is available in the MACTAS’ official code repository in the file `requirements.txt`.

G Hardware

Here we present the hardware used in our experiments. We utilized the NVIDIA Ampere GPU architecture across three computational clusters. The specific setup is presented in Table 6.